



HAL
open science

Non-ionic deep eutectic solvents for membrane formation

Norafiqah Ismail, Jun Pan, Mahmoud Rahmati, Qian Wang, Denis Bouyer, Mohamed Khayet, Zhaoliang Cui, Naser Tavajohi

► **To cite this version:**

Norafiqah Ismail, Jun Pan, Mahmoud Rahmati, Qian Wang, Denis Bouyer, et al.. Non-ionic deep eutectic solvents for membrane formation. *Journal of Membrane Science*, 2022, 646, pp.120238. 10.1016/j.memsci.2021.120238 . hal-03929808

HAL Id: hal-03929808

<https://hal.umontpellier.fr/hal-03929808v1>

Submitted on 21 Oct 2023

HAL is a multi-disciplinary open access archive for the deposit and dissemination of scientific research documents, whether they are published or not. The documents may come from teaching and research institutions in France or abroad, or from public or private research centers.

L'archive ouverte pluridisciplinaire **HAL**, est destinée au dépôt et à la diffusion de documents scientifiques de niveau recherche, publiés ou non, émanant des établissements d'enseignement et de recherche français ou étrangers, des laboratoires publics ou privés.



Distributed under a Creative Commons Attribution - NonCommercial - NoDerivatives 4.0 International License



Non-ionic deep eutectic solvents for membrane formation

Norafiqah Ismail^a, Jun Pan^b, Mahmoud Rahmati^c, Qian Wang^b, Denis Bouyer^d,
Mohamed Khayet^{e,f}, Zhaoliang Cui^{b,**}, Naser Tavajohi^{a,*}

^a Department of Chemistry, Umeå University, 90187, Umeå, Sweden

^b State Key Laboratory of Materials-Oriented Chemical Engineering, College of Chemical Engineering, Nanjing Tech University, Nanjing, 211816, PR China

^c Department of Chemical Engineering, Graduate University of Advanced Technology, Kerman, Iran

^d Institut Européen des Membranes, IEM, UMR 5635, ENSCM, CNRS, Univ Montpellier, Montpellier, France

^e Department of Structure of Matter, Thermal Physics and Electronics, Faculty of Physics, University Complutense of Madrid, Avda. Complutense S/n, 28040, Madrid, Spain

^f Madrid Institute for Advanced Studies of Water (IMDEA Water Institute), Calle Punto Net N° 4, 28805, Alcalá de Henares, Madrid, Spain

ARTICLE INFO

Keywords:

Deep eutectic solvent
Polyvinylidene fluoride
Biodegradable
Membrane preparation

ABSTRACT

Deep eutectic solvents (DES) have recently emerged as a new class of inexpensive biodegradable solvents and additives with diverse applications. In this study, a new family of non-ionic deep eutectic solvents (NIDES) is proposed for the first time for membrane preparation. Three types of NIDES, N-methylacetamide-acetamide (DES-1), N-methyl acetamide-N-methyl urea (DES-2), and N-methyl acetamide-N,N'-dimethyl urea (DES-3) were synthesized and used to dissolve polyvinylidene fluoride (PVDF) polymer. The effects of the additive polyvinylpyrrolidone (PVP) and the type of NIDES on the PVDF membrane characteristics, water permeability and bovine serum albumin (BSA) separation were studied. The membranes prepared with DES-1 and 2 wt% PVP exhibited a good water permeate flux (96.82 L/m².h) and a high BSA separation factor (96.32%). High performance PVDF membranes can thus be efficiently prepared using biodegradable inexpensive NIDES.

1. Introduction

Solvents are ubiquitous in chemistry. They are generally used to bring species together for reactions, separations of species, materials processing or cleaning. However, the solvents most commonly used in chemical processes are volatile organic compounds (VOCs) whose use cause significant environmental problems and limits process sustainability. Additionally, the properties of solvents used in the fabrication of materials can strongly influence the processability of their production lines and hence affect their scaling-up, cost and practical use as consequence. For instance, some advanced polymeric materials cannot yet be used in real-world applications due to their limited processability. Nevertheless, polymeric materials are a major pillar of the world economy and are used extensively in a numerous variety of products ranging from food and beverage containers to automotive components. Some applications such as membrane separation require polymeric materials with high thermal, chemical, and mechanical robustness. Fluorinated polymers satisfy these requirements but are poorly soluble in many common solvents and are therefore frequently processed in toxic organic

solvents, which limits the sustainability of their fabrication. Consequently, there is a clear need to identify biodegradable and green solvents suitable for processing of polymeric materials.

In addition to being able to dissolve polymers and additives while retaining good processability, solvents used in membrane fabrication must be compatible with the phase inversion technique, which has become the dominant membrane fabrication technique in industry and academia since its invention by Loeb and Sourirajan in 1963 [1]. In this case, a given quantity of polymer is dissolved in an appropriate solvent or in a mixture of solvents, after which a phase inversion is induced by the action of an internal factor (e.g. solvent evaporation) or by an external factor (e.g. temperature variation, addition of a nonsolvent, introduction of an appropriate vapor). Nonsolvent-induced phase separation (NIPs) and thermally-induced phase separation (TIPs) are currently the most followed procedures for polymeric membrane fabrication [2]. It must be pointed out that both the thermodynamics and kinetics of the phase inversion technique are strongly dependent on the properties of the used solvent(s). Although several solvents can dissolve certain polymers and achieve an acceptable processability, very few

* Corresponding author.

** Corresponding author.

E-mail addresses: zcui@njtech.edu.cn (Z. Cui), naser.tavajohi@umu.se (N. Tavajohi).

<https://doi.org/10.1016/j.memsci.2021.120238>

Received 12 November 2021; Received in revised form 28 December 2021; Accepted 29 December 2021

Available online 3 January 2022

0376-7388/© 2022 The Authors.

Published by Elsevier B.V. This is an open access article under the CC BY-NC-ND license

(<http://creativecommons.org/licenses/by-nc-nd/4.0/>).

solvents are suitable for large-scale membrane fabrication. It is also important noting that, even though TIPs method allows a broader selection of polymer and solvent, higher energy consumption than NIPs is required for the preparation of a homogenous polymer solution.

Table 1 lists several solvents that have been successfully used in membrane fabrication. All these solvents both dissolve the target polymer and enable the fabrication of membranes with a specific desired morphological structure. However, the disposal of these solvents presents significant problems. Razali et al. [3] reported over 50 million liters of solvents are discharged into the environment annually, and most of the widely used solvents in the membrane fabrication industry are toxic and negatively impact human health and the environment. For instance, N-methylpyrrolidone (NMP) can cause reproductive disorders and its use has been banned in Europe since May 2020. Moreover, dioctyl phthalate (DOP) is a human carcinogen and dibutyl phthalate (DBP) can cause fetal malformation [4,5]. Moreover, many of these solvents are VOCs and are thus toxic, volatile, and flammable.

Various green and biodegradable solvents have been proposed during last two decades for membrane production as shown in Table 2. Some of these green solvents such as Polarclean [6] and Cyrene™ [7] are commercially available. The ongoing development of ionic liquids (ILs) as alternative sustainable solvents is also noteworthy. ILs are non-flammable and have a relatively low vapor pressures making them

attractive alternatives to toxic conventional solvents. However, many ILs are based on imidazolium and pyridinium cations that are not fully environmentally benign because they are synthesized from petrochemicals, which show a wide range of toxicities towards microorganism, vertebrates and invertebrates due to their poor degradability [8]. Even though the low vapor pressure of IL brings a good advantage over typical VOC solvents, the release of ILs from industrial processes into aquatic environments may lead to water pollution because of their high water solubility. Moreover, their synthesis generally requires large quantities of salts and solvents to complete the anions exchange process. These drawbacks together with the high cost of common ILs unfortunately restrict their use in emerging industries [9,10].

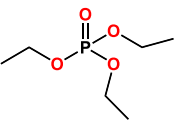
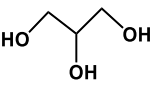
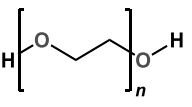
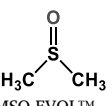
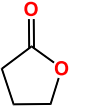
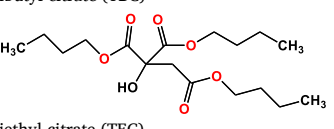
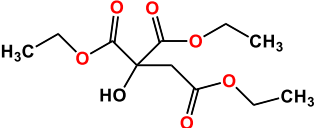
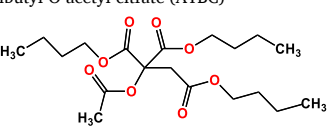
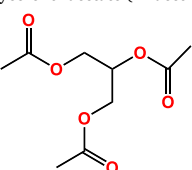
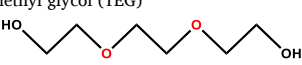
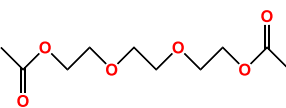
More recently, a family of novel solvents known as deep eutectic solvents (DES) was identified as an alternative to ILs. DES are synthesized by simple green methods [11] that require non-toxic components and do not generate any byproducts [12]. DES are formed by mixing hydrogen bond acceptors and donors in a stoichiometric ratio, leading to intermolecular hydrogen bond association melting [13]. These recently developed solvents could potentially allow conventional VOCs to be replaced with safer, greener liquids whose intriguing properties offer significant advantages in membrane preparation. It is worthwhile, to consider that the cost, toxicity and biodegradability of DES depend on the selected type of chemicals providing the hydrogen donor and

Table 1

List of solvents used in membrane fabrication.

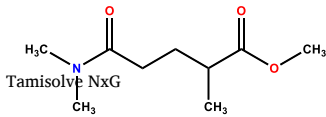
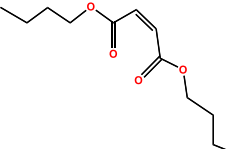
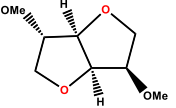
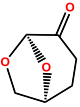
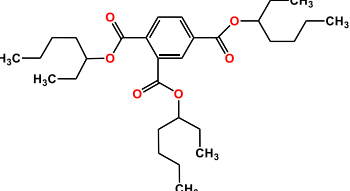
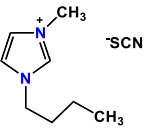
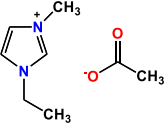
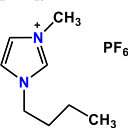
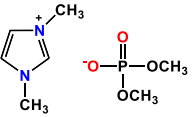
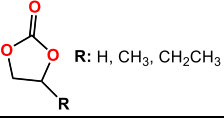
Solvent	Polymer type	Configuration	Year	Reference
Mineral oil, Kel-F oligomer oil, dibutyl phthalate (DBP)	Polypropylene (PP), high density polyethylene (HDPE), poly(4-methyl-1-pentene)(TPX), PVDF	Flat sheet	1990	Lloyd et al. [18]
N,N-bis (2-hydroxyethyl) Tallowamine	iPP	Flat sheet	1991	Lloyd et al. [19]
Eicosane, eicosanoic acid, N,N-bis (2-hydroxyethyl) Tallowamine	iPP	Flat sheet	1991	Kim et al. [20]
Mineral oil, eicosane, tetradecane, dotriacontane	iPP	Flat sheet	1991	Gordon et al. [21]
Tetradecane, dotriacontane, pentadecanoic acid, eicosane, eicosanoic acid	iPP	Flat sheet	1991	Kim et al. [22]
Hexamethylbenzene (HMB)	iPP	Flat sheet	1991	Alwattari et al. [23]
Dotriacontane	iPP	Flat sheet	1993	McGuire et al. [24]
Diphenyl ether (DPE)	iPP	Flat sheet	1994	Laxminarayan et al. [25]
	iPP	Flat sheet	1994	McGuire et al. [26]
	iPP	Flat sheet	1996	McGuire et al. [27]
	iPP	Flat sheet	2000	Matsuyama et al. [28]
	Syndiotactic polypropylene (sPP)	Flat sheet	2005	Yave et al. [29]
	iPP, sPP	Flat sheet	2005	Yave et al. [30]
Chlorotrifluoroethylene	Poly(tetrafluoroethylene-co-perfluoro-(propylvinyl ether) (Teflon PFA)	Flat sheet	1997	Caplan et al. [31]
Diisodecyl phthalate (DIDP), LP	HDPE	Hollow fiber	2003	Matsuyama et al. [32]
DBP, DOP	iPP	Hollow fiber	2006	Yang et al. [33]
DBP, DOP	iPP	Hollow fiber	2006	Yang et al. [34]
Dioctylsebacate (DOS), DOP and dimethyl-phthalate (DMP)	PVDF	Flat sheet	2006	Gu et al. [35]
DMP	PVDF	Flat sheet	2006	Gu et al. [36]
Butyrolactone, cyclohexane (CO), DBP	PVDF	Flat sheet	2007	Su et al. [37]
Butyrolactone, propylene carbonate (PC), DBP, dibutyl sebacate (KD)	PVDF	Flat sheet	2007	Su et al. [38]
DBP, di(2-ethylhexyl) phthalate (DEHP)	PVDF	Flat sheet	2008	Ji et al. [39]
DBP, DEHP, LP	PVDF	Hollow fiber	2008	Ji et al. [40]
Diphenylketone (DPK)	PVDF	Flat sheet	2008	Yang et al. [41]
	Poly phenylene sulfide (PPS)	Flat sheet	2008	Han et al. [42]
DBP	PVDF	Flat sheet	2008	Li et al. [43]
DBP,DOP	PVDF	Flat sheet	2009	Lu et al. [44]
DPC	PVDF	Flat sheet	2009	Lin et al. [45]
	PVDF	Hollow fiber	2016	Lin et al. [46]
Diamyl phthalate (DAP)	iPP	Flat sheet	2009	Lin et al. [47]
DPK, 1,2-propylene glycol (PG)	PVDF	Flat sheet	2010	Tang et al. [48]
Methyl salicylate (MS), benzophenone (BP)	PVDF/poly methyl methacrylate (PMMA)	Flat sheet	2011	Ma et al. [49]
Diethyl phthalate (DEP)	PVDF	Hollow fiber	2012	Rajabzadeh et al. [50]
NMP	PVDF	Flat sheet	2015	Xu et al. [51]
Dioctyl adipate (DOA)	ECTFE	Flat sheet	2015	Pan et al. [52]

Table 2
Green solvents used in membrane fabrication.

Solvent	Polymer type	Configuration	Year	Reference
Triethyl phosphate (TEP)	PVDF PVDF	Flat sheet Hollow fiber	1991 2012	Bottino et al. [53] Abed et al. [54]
				
Liquid paraffin (LP)	HDPE	Hollow fiber	2000	Sun et al. [55]
Glycerol	Poly(ethylene-co-vinyl alcohol)(EVOH)	Hollow fiber	2003	Shang et al. [56]
				
Polyethylene glycol (PEG)	PVB PVB, EVOH PVB/Pluronic F127 PVB/Pluronic F127	Hollow fiber Hollow fiber Hollow fiber Hollow fiber	2005 2006 2008 2009	Fu et al. [57] Fu et al. [58] Qiu et al. [59] Qiu et al. [60]
				
Dimethyl sulfoxide (DMSO)	PVDF PVDF/PMMA	Flat sheet Flat sheet	2012 2006	Wang et al. [61] Lin et al. [62]
				
DMSO EVOL™ γ-Butyrolactone (γ-BL)	PES PVDF PEEK-WC	Flat sheet Hollow fiber Hollow fiber	2019 2012 2011	Marino et al. [4] Song et al. [63] Bey et al. [64]
				
Tributyl citrate (TBC)	PVDF	Flat sheet	2010	Liu et al. [65]
				
Triethyl citrate (TEC)	Poly(ethylene chlorotrifluoroethylene) (ECTFE)	Hollow fiber	2005	Mullette et al. [66]
				
Tributyl O-acetyl citrate (ATBC)	PVDF	Flat sheet and hollow fiber	2013	Cui et al. [2]
				
Mineral oil Glycerol triacetate (Triacetin)	UHMWPE PVDF/PMMA PVDF PVDF PVDF ECTFE	Hollow fiber Hollow fiber Hollow fiber Hollow fiber Flat sheet	2011 2009 2010 2011 2012 2014	Li et al. [67] Rajabzadeh et al. [68] Rajabzadeh et al. [69] Ghasem et al. [70] Ghasem et al. [71, 72] Drioli et al. [73]
				
Triethyl glycol (TEG)	Cellulose acetate butyrate (CAB) Cellulose acetate (CA), CAB, Cellulose acetate propionate (CAP)	Hollow fiber Hollow fiber	2008 2011	Fu et al. [74] Shibutani et al. [75]
				
Triethylene glycol diacetate (TEGDA)	PVDF	Flat sheet	2015	Cui et al. [76]
				
	PVDF PES	Hollow fiber Flat sheet	2015 2018	Hassankiadeh et al. [6] Marino et al. [77]

(continued on next page)

Table 2 (continued)

Solvent	Polymer type	Configuration	Year	Reference
Methyl-5-(dimethylamino)-2-methyl-5-oxopentanoate (Polarclean)				
				
Maleic acid dibutyl ester (DBM)	P(VDF-HFP) PVDF	Flat sheet Flat sheet	2017 2018	Marino et al. [78] Cui et al. [79]
				
Dimethyl Isosorbide	PVDF	Flat sheet	2019	Russo et al. [80]
				
Cyrene™	PES, PVDF	Flat sheet	2019	Marino et al. [7]
				
Trioctyl trimellitate (TOTM)	ECTFE	Flat sheet	2020	Liu et al. [81]
				
1-butyl-3-methylimidazolium ([BMIM]SCN)	CA	Hollow fiber and flat sheet	2010	Xing et al. [82]
				
1-ethyl-3-methylimidazolium acetate ([EMIM]OAc)	Polybenzimidazole (PBI)	Flat sheet	2014	Xing et al. [83]
				
1-butyl-3-methylimidazolium hexafluorophosphate ([BMIM][PF6])	PES PVDF	Flat sheet Flat sheet	2015 2020	Lakshmi et al. [84] Wang et al. [85]
				
1,3-dimethylimidazolium dimethyl phosphate ([MMIM]DMP)	PES	Flat sheet	2017	Kim et al. [86]
				
Cyclic carbonates	PVDF	Flat sheet	2021	Ismail et al. [87]
				

hydrogen acceptor. By choosing adequate types of hydrogen donor and hydrogen acceptor one can synthesize competitive DES for membrane fabrication.

Previously reported studies on DES in membrane fabrication have focused on their use as additives. For example, Bin Jiang et al. [14] found that a DES formed by mixing tetrabutylammonium chloride and decanoic acid in a molar ratio of 1:2 enhanced pore formation of the prepared membrane. This was attributed to the unique structure of the used DES and water solubility properties. Another study showed that a series of imidazole-based DES can serve as functional additives to improve the performance of polyethersulfone (PES) membranes [15]. Vatanpour et al. [16] introduced the hydrophilic DES ethaline, which is a mixture of choline chloride and ethylene glycol at a molar ratio of 1:2 in PES/dimethyl acetamide (DMAC) polymer solution. Their results showed that DES can be used as hydrophilic additives to enhance membranes' antifouling properties.

In this study we present the first assessment of the potential of non-ionic DES (NIDES) as alternative, cheap, less toxic, biodegradable, and scalable solvents for membrane fabrication. The synthesized NIDES are proposed to dissolve the fluoropolymer polyvinylidene fluoride (PVDF), which is among the most widely used polymers in membrane fabrication by phase inversion technique. PVDF is used in several industries including electronics, biomedical, piping, and coating because it has favorable thermochemical and mechanical properties while also displaying excellent processability [17].

2. Experimental

2.1. Materials

Acetamide (AA), N-methylacetamide (NMA), N-methylurea (NMU), and N,N'-dimethylurea (NN'-DMU) were purchased from TCI Europe. PVDF (1015, powder) was kindly provided by Solvay Specialty Polymers. Polyvinylpyrrolidone (PVP, K-17, MW: 9000 g/mol) was used as a pore forming agent of PVDF membranes. Kerosene, used for the measurement of the membrane porosity, was purchased from Sigma Aldrich.

Bovine serum albumin (BSA, MW: 67 kDa) purchased from Sigma Aldrich was used to study the rejection rate of the prepared PVDF membranes.

2.2. Synthesis of non-ionic deep eutectic solvents (NIDES)

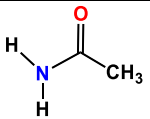
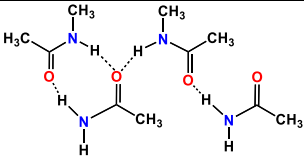
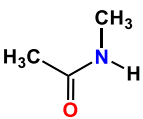
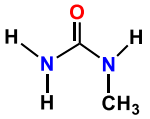
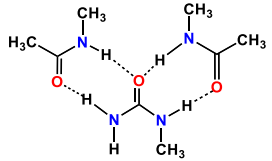
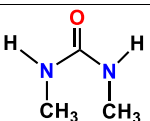
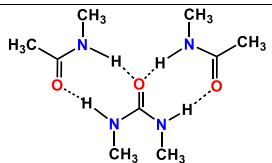
The eutectic mixtures were prepared by heating a known amount of NMA at 40 °C until a clear liquid was obtained. The appropriate quantity (w/w) of the other component, AA (30%), NMU (20%), or NN'-DMU (30%) was then added to the molten NMA and the mixture was stirred until a homogenous phase was formed. Table 3 shows the chemical structures of the used compounds and the expected final structures of the synthesized NIDES.

2.3. Molecular dynamics simulations, solubility parameters and phase diagrams of NIDES systems

Molecular dynamics (MD) simulations were performed using Materials Studio (BIOVIA Accelrys, version 4.3). The initial density of the DES solvent molecules was fixed at 0.5 g/cm³ [88]. Each simulation had a duration of 1 ns with a 1 fs time step and a cut-off radius of 12.5 Å for short-range non-bonded interactions. The Ewald summation method was used to estimate long-range interactions with an accuracy of 0.001 kcal mol⁻¹ [89]. The NPT ensemble (*i.e.* with a constant number of molecules, temperature, and pressure) was used to calculate the density and solubility parameters of the solutions at 298 K and 1 bar. The temperature and pressure were kept constant using the Nose-Hoover thermostat with a Q ratio of 0.005 and a relaxation time of 0.1 ps and the Anderson barostat with a decay of 0.5 ps, respectively. Periodic boundary conditions were applied to the simulation boxes [90].

A crucial aspect of any simulation is the choice of a force field. It must be mentioned that the force fields commonly consider a combination of internal coordinates and the terms (bond distances, bond angles, torsions, etc.) to describe the contributions of interactions between bonded atoms to the potential energy hypersurface, while non-bond terms are used to describe non-covalent interactions between atoms

Table 3
Solvent mixtures used in this study.

First solvent	Second solvent	Expected final structure
	 Acetamide (AA)	 DES-1
 N-methylacetamide (NMA)	 N-Methylurea (NMU)	 DES-2
	 N,N'-Dimethylurea (N,N'-DMU)	 DES-3

including van der Waals and electrostatic interactions. Condensed-phase optimized molecular potentials for atomistic simulation studies (COMPASS) represents a major advancement in the development of force field methods [91] because it is the first *ab initio* force field enabling accurate simultaneous prediction of both gas-phase properties (including structural, conformational, and vibrational properties) and condensed-phase properties (e.g., equations of state and cohesive energies) for a broad range of molecules and polymers [92]. In addition, it is also the first high quality force field to consolidate parameters for organic and inorganic materials. Taking into consideration these capabilities, COMPASS has been widely used to model interactions between solvent molecules [89]. Therefore, it was employed in the present study to analyze the interactions between AA, NMU, NMA and N,N'-DMU molecules.

The accuracy of the simulations was evaluated by computing the solubility parameters and cohesive energy densities of the solutions. The solubility parameter, δ , plays an important role in the theory of mixtures and it is defined as [88,93]:

$$\delta = \sqrt{CED} \quad (1)$$

where CED is the cohesive energy density defined as the cohesive energy per unit of volume [88]:

$$CED = \frac{E_{coh}}{V} \quad (2)$$

The cohesive energy of a system of molecules, E_{coh} , is the average energy required to separate all molecules to an infinite distance from each other:

$$E_{coh} = -E_{inter} = E_{intra} - E_{total} \quad (3)$$

where E_{inter} is the total energy of the interactions between all molecules, which is equal to the total energy of the system, E_{total} , minus the intramolecular energy, E_{intra} . The brackets indicate averages over an NPT (constant pressure and constant temperature) ensemble.

The simulation results were further analyzed by performing radial distribution function (*RDF*) analysis. *RDF* analysis has been used to investigate the interactions and accumulation of solution molecules under different conditions. The radial pair distribution function for two particle types *a* and *b* is:

$$g_{ab}(r) = (N_a N_b)^{-1} \sum_{i=1}^{N_a} \sum_{j=1}^{N_b} \delta(|r_i - r_j| - r) \quad (4)$$

This expression is normalized such that the *RDF* becomes 1 for large separations in an homogenous system. The *RDF* effectively counts the average number of 'b' neighbors in a shell of radius *r* centered on an 'a' particle and represents it as a density.

The solubility parameter δ is related with the contributions of the dispersive interactions (δ_d), the interactions between permanent dipoles (i.e. the polar term, δ_p), and the hydrogen bonding (δ_H) [94]:

$$\delta = \sqrt{\delta_d^2 + \delta_p^2 + \delta_H^2} \quad (5)$$

The solubility parameter of each component is calculated by means of the group contribution method following the same procedure reported in Rasool et al. [95]. Hansen solubility parameters values for each component of a polymer/solvent system are calculated as follows:

$$\delta_d = \frac{\sum F_{di}}{\sum V} \quad (6)$$

$$\delta_p = \frac{\sum \sqrt{F_{pi}^2}}{\sum V} \quad (7)$$

$$\delta_H = \sqrt{\frac{\sum E_{hi}}{\sum V}} \quad (8)$$

where F_{di} , F_{pi} and E_{hi} are the parameters for dispersion forces, polar forces and hydrogen bonding forces, respectively. This method is also known as the Hoftyzer Van Krevelen method [96].

The polymer-solvent interaction parameter is calculated by using Flory-Huggins interaction parameter which expanded with Hansen solubility parameter using the following equation:

$$\chi = \frac{V_s}{RT} \left[(\delta_{d,p} - \delta_{d,s})^2 + 0.25(\delta_{p,p} - \delta_{p,s})^2 + 0.25(\delta_{h,p} - \delta_{h,s})^2 \right] \quad (9)$$

where V_s is the molar volume of the solvent, δ_p and δ_s are the solubility parameter of the polymer and solvent respectively. R is the gas constant (8.3145 J mol⁻¹ K⁻¹) and T is the temperature in K. All the calculation for solubility parameters are presented in Supporting information.

The phase diagram of a polymer/solvent system is an important tool for understanding its phase separation behavior from thermodynamic perspective. To generate phase diagrams for the PVDF/NIDES systems studied in this work, solutions were prepared at five different polymer concentrations (i.e., 10, 12.5, 15, 17.5, and 20 wt%) for each studied solvent system.

The cloud point was observed and measured by placing the sample under microscope (XPV-800E, BIMU, Shanghai, China). The sample was place in between of microscope slide to prevent solvent evaporation. Then sample were heated up for 200 °C and kept for 5 min when it completely turned to transparent. Then, the sample was cooled down to 20 °C with a constant rate of 6 °C/min. The temperature of cloud point was recorded once the sample turned to turbid. The average of temperature for 5 times repetitions were used as final cloud point.

A differential scanning calorimetry (DSC, Q20, TA instrument, DE, USA) was used to measure crystallization temperature. The sample was weight first for 5 mg and then heated up to 250 °C. Secondly, the sample was cooled down to 10 °C at cooling rate of 10 °C/min to obtain crystallization temperature.

2.4. Membrane preparation

The dope solution was prepared by adding PVP to NMA-AA, NMA-NMU or NMA-N,N'-DMU solution at 40 °C. PVDF was then added and the solution was stirred continuously at 140 °C until a homogenous dope solution was formed. For all NIDES, the PVDF concentration was 15 wt %, while the PVP concentration was 2 wt%. This PVP concentration was selected taking into consideration the optimum filtration performance of the PVDF membranes prepared with DES-1 and different PVP concentrations varying from 0 to 4 wt%.

Flat-sheet membranes were cast at an elevated temperature 140 °C. A casting system, purchased from Elcometer Ltd., was used and the membrane thickness was fixed at 250 μm. After casting, the cast films were immediately immersed in a coagulation bath filled with distilled water at 45 °C and kept for 1 day before being immersed in ethanol for another day to completely remove any residual solvents. The use of the above indicated high temperature to prepare the polymer solution and the membrane increases the energy consumption and the subsequent membrane cost. Life cycle assessment (LCA) study and cost effectiveness analysis should be performed for this type of membrane and comparisons to other TIPs and NIPs membranes should be made taking into consideration all involved materials and their costs and environmental impacts. For sake of comparison, a PVDF membrane without PVP additive was prepared under the same conditions. The prepared membranes are named hereafter, PVDF/xPVP/DES-y, where *x* refers to the concentration of PVP and *y* is the type of NIDES (e.g. PVDF/2PVP/DES-3 is the PVDF membrane prepared with 2 wt% PVP and the solvent DES-3, and PVDF/DES-1 is the PVDF membrane prepared without PVP and the solvent DES-1).

2.5. Membrane characterization

Nuclear magnetic resonance (^1H NMR) spectroscopy was performed using a Bruker Avance 400 MHz NMR equipment to determine the chemical structure of the studied NIDES. All NMR spectra were assigned using Bruker's Topspin processing software. $\text{DMSO-}d_6$ was used as an internal standard and a solvent in the performed analysis.

The infrared spectra of the fabricated membranes were acquired using a Bruker Vertex 80 spectrometer in the range of $600\text{--}1600\text{ cm}^{-1}$ with a resolution of 2 cm^{-1} in ATR (attenuated total reflection) mode.

Density of the NIDES solution was measured using Mettler Toledo DA-110 m density meter at room temperature. The samples were taken three times to measure the average value.

A Field Emission Scanning Electron Microscope (FE-SEM) from Carl Zeiss was used to obtain images of membrane surfaces and their cross-sections. First, the membrane samples were freeze-fractured in liquid nitrogen. Then all samples were coated with a 5 nm thick palladium layer using a Quorum Q150T-ES Sputter Coater. The membrane thickness was measured simultaneously after obtaining cross-section images. The measurement was taken 3 times of 3 different spots.

Permeability tests were conducted at room temperature using a dead-end Amicon stirred cell. The water permeate flux of the membranes was measured under a *trans*-membrane pressure of 1 bar. The effective diameter of the membrane filtration area was 43 mm. Due to the hydrophobic character of the PVDF membranes, these were immersed in an ethanol solution for 1 day and then washed with water prior to filtration tests. All membranes were compacted using distilled water and applying a hydrostatic pressure of 1 bar for 10 min until a stable permeate flux is established. The average water permeate flux was obtained by measuring the water permeate flux of three membrane samples prepared under identical fabrication conditions. The water permeability ($\text{L}/\text{m}^2\cdot\text{h}\cdot\text{bar}$) of each membrane was determined using the following expression:

$$PWP = \frac{J}{A \cdot t} \quad (10)$$

where J is the volume of water permeated through the membrane (L), A is the effective filtration area of the membrane (m^2), and t represents the time corresponding to a certain volume of collected water (h).

The separation performance of the prepared membranes was studied using as feed 1000 ppm bovine serum albumin (BSA) aqueous solution. The aqueous feed solution (BSA) was stirred magnetically to minimize the concentration polarization effect. The BSA rejection factor was calculated using Eq. (11):

$$BSA \text{ rejection } (\%) = \left(1 - \frac{C_p}{C_f}\right) \times 100 \quad (11)$$

where C_f and C_p are the initial feed and permeate concentrations of BSA, respectively. BSA concentrations in the feed and permeate were determined by UV-Vis spectrophotometry at a wavelength of 280 nm.

XRD spectra of the membrane samples were obtained with a PANalytical X'Pert PRO X-ray diffractometer operated at 40 kV and 40 mA using $\text{Cu-K}\alpha$ radiation at a wavelength of 0.154 nm. The samples were scanned in a 2θ range of $10^\circ\text{--}40^\circ$ at a rate of $0.5^\circ/\text{min}$. A silicon-based specimen holder was used in these experiments and the $1/2^\circ$ divergence slit size was fixed in all measurements.

For membrane porosity measurements, the weight of the dry samples were measured first, then the same samples were immersed in kerosene for 24 h and their wet weights were measured. The overall membrane porosity was calculated using the following equation:

$$\varepsilon (\%) = \frac{\frac{(m_w - m_d)}{\rho_w}}{\frac{(m_w - m_d)}{\rho_w} + \frac{m_d}{\rho_p}} \times 100\% \quad (12)$$

where m_w and m_d are the weights of the wet and dry membranes,

respectively, while ρ_w and ρ_p are the densities of kerosene and the polymer, 0.81 and $1.78\text{ g}/\text{cm}^3$, respectively.

The average pore size (r_m) is calculated by The Guerout-Elford-Ferry equation, which is expressed as follows:

$$r_m = \sqrt{\frac{(2.9 - 1.75\varepsilon) \times 8\mu Q}{\varepsilon \times A \times \Delta P}} \quad (13)$$

and the membrane resistance is calculated according to Darcy's law

$$R = \frac{\Delta P}{\mu \cdot PWP} \quad (14)$$

where ε , porosity (%), μ viscosity of water ($8.9 \times 10^{-4}\text{ Pa s}$), l is the thickness in mm, Q is the volume per second (m^3/s), A is the membrane area (m^2), ΔP is the operational pressure (Pa).

The membrane contact angle was analyzed using a Theta Optical Tensiometer at room temperature. 4 μL distilled water was placed on the membrane surface in each measurement.

The mechanical properties (tensile strength and elongation at break) of the membranes were studied using a tensile testing instrument (HLD 1000, China). For each membrane, 5 samples were tested and the average values together with their standard deviations were reported. More details about the above mentioned characterization techniques can be found elsewhere [97].

3. Results and discussions

3.1. Characteristics of synthesized NIDES

The NIDES is a mixture of two or more components that forms an eutectic with a eutectic point below that of any of its individual components. The phase diagrams of the three proposed NIDES for membrane preparation in this study are presented in Fig. 1a. Each NIDES was synthesized by mixing NMA (the first component) with either AA, NMU or N'-DMU. At room temperature, all these components are in liquid phase. However, the proposed NIDES by mixing them are liquids (Fig. 1b). The ^1H NMR and FTIR spectra of NMA and the three NIDES are shown in Fig. 1c and d, respectively. These indicate that the individual components of each NIDES retained its initial molecular structure, which is consistent with the findings of previous studies on DES [98–100].

MD simulations were performed to investigate the chemical structure of the synthesized NIDES. The density and solubility parameters of DES-1, DES-2 and DES-3 solutions obtained from these simulations are listed in Table 4. As can be seen, the MD simulated density agree well with the experimental data within less than 4.2%. In addition, the obtained values of the total solubility parameters by MD simulations were underestimated by a maximum of 8.3% compared to those calculated by means of the group contribution method confirming the reasonably good agreements between them.

Due to the presence of N and O atoms in the structures of NMA, AA, NMU and N',N'-DMU molecules, hydrogen bonding between the components of the NIDES is expected. Fig. 2a shows a schematic depiction of DES-1 at the end of the simulation in which the pink dashed lines indicate hydrogen bonds between NMA and AA molecules. These can be seen clearly in Fig. 2b, in which only the hydrogen bonds between these molecules are shown. These figures indicate that the results of the MD simulations strongly suggest the presence of extensive hydrogen bonding within the synthesized NIDES solutions.

The hydrogen bonding between N and O atoms of the NIDES components and their N-H groups was also investigated based on RDF analyses. Fig. 2c and d show the RDFs for O-H and N-H interactions, respectively. The O-H RDF exhibits a sharp peak at 1.9 \AA indicating the presence of a strong hydrogen bonding in the three NIDES solutions. The highest peak intensity was found for DES-3 whereas the lowest one was registered for DES-1. On the contrary, no sharp peak below 2 \AA was

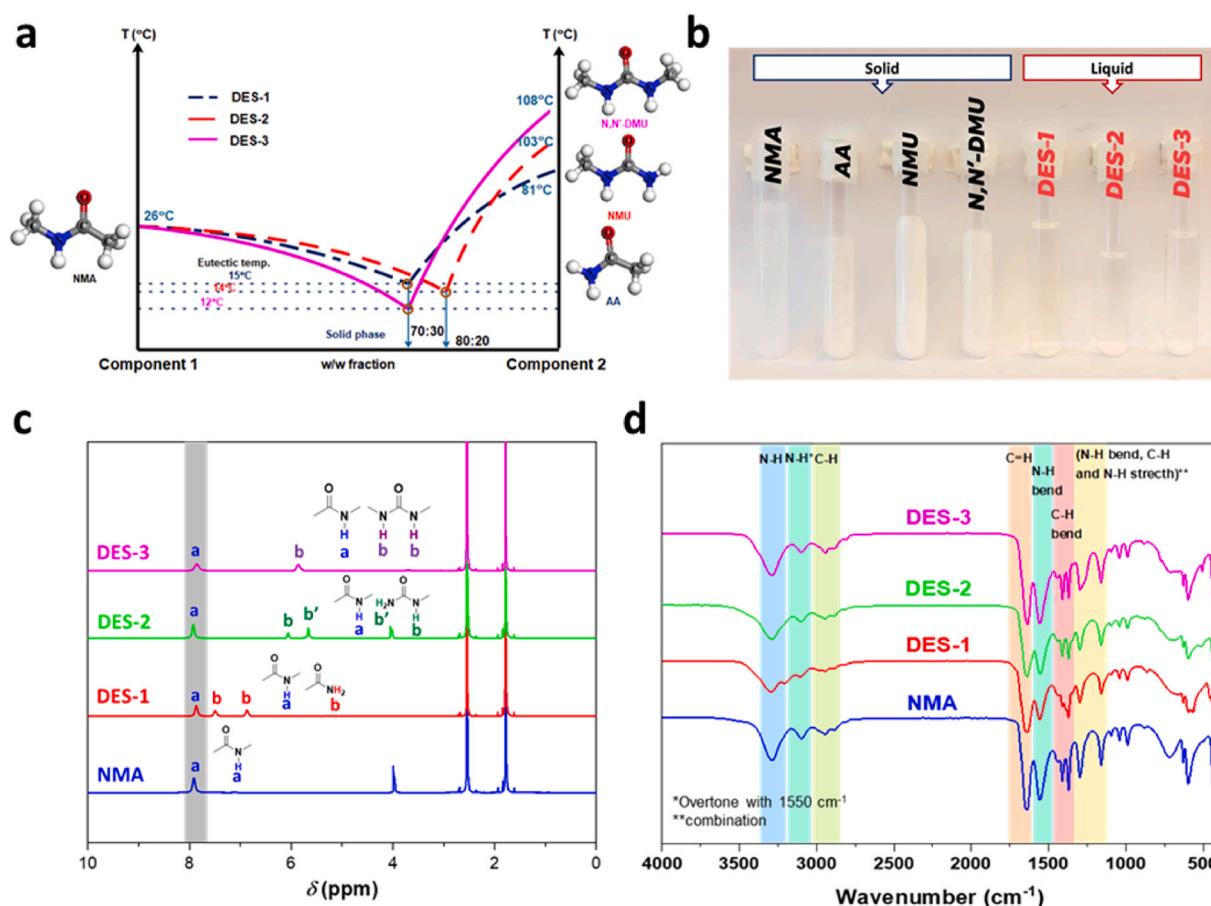


Fig. 1. a) Phase diagrams of the proposed NIDES, b) photos of the used components (NMA, AA, NMU and N,N'-DMU) and the synthesized NIDES solutions (DES-1, DES-2 and DES-3), c) ^1H NMR spectra, and d) FTIR spectra*

Note: The values of the eutectic points shown in Fig. 1a are obtained from Nzideye et al. [13].

detected for the RDF of N–H (Fig. 2d) indicating that hydrogen bonds between N and H atoms are longer than those between O and H atoms. These results point out that O–H hydrogen bonding is stronger than N–H hydrogen bonding, which is consistent with the structures presented in Table 3. Furthermore, based on its higher radial pair distribution ($g(r)$) and the greater number of hydrogen bonds formed within its simulated box (164), DES-3 appears to have stronger hydrogen bonds than the other two studied NIDES. This result is consistent with the finding that DES-3 exhibits the lowest eutectic point among the three proposed NIDES (see Fig. 1a).

Apart from simple and inexpensive synthesizing process, a major advantage of the NIDES solvents is their low viscosity compared to that of ionic liquids (ILs). This parameter is crucial for polymer solution processability and highly concentrated polymer solutions can be prepared.

3.2. Solubility and phase diagram of PVDF/NIDES systems

The group contribution method was used to estimate the solubility parameter of PVDF in the three different NIDES solvents. Based on the Hansen solubility sphere illustrated in Fig. 3a, PVDF was not expected to be soluble in any of the proposed NIDES. However, the performed experimental results showed that PVDF could be dissolved in these mixtures at 140 $^{\circ}\text{C}$. This can be attributed to the increased solvation power of NIDES solvents at higher temperatures. It was therefore concluded that the group contribution method is not optimal for assessing its suitability for PVDF membrane preparation, especially for TIPS technique.

Phase diagrams reflect thermodynamics properties such as the mutual affinity between polymer and solvent, which is an essential parameter to consider when fabricating membranes by the phase inversion technique. Because the proposed NIDES cannot dissolve PVDF at room temperature, higher temperatures are needed to induce phase separation. Fig. 3b, c and 3d show both the cloud point and crystallization temperatures for different PVDF concentrations in the three PVDF/NIDES systems, PVDF/DES-1, PVDF/DES-2 and PVDF/DES-3, respectively. These figures show that the cloud point and crystallization temperature curves do not intersect at any polymer concentration below 20 wt%, indicating that liquid-liquid (L-L) separation will occur for the PVDF concentrations in this range. The three polymer/solvents systems have L-L separation region in which the PVDF-solvent interaction (χ) value is high (Table 4) indicating weak polymer-solvent interactions. It should be noted that solid-liquid separation may occur in regions with low χ (good polymer-solvent interactions) when the polymer concentration is high, but L-L separation will not occur under such conditions because of the relatively flat binodal curves of the three systems.

The PVDF/DES-3 system has a lower crystallization temperature than the other systems PVDF/DES-1 and PVDF/DES-2. This is as expected since the χ value of the PVDF/DES-3 is lower compared to that of PVDF/DES-1 and PVDF/DES-2. In addition, PVDF/DES-2 has a slightly higher crystallization temperature than PVDF/DES-1, which is consistent with the obtained χ values (i.e. χ value of PVDF/DES-1 is lower than that of PVDF/DES-2). It is known that in TIPS technique, L-L phase separation results in the formation of membranes with a cellular morphological structure, whereas solid-liquid phase inversion induces

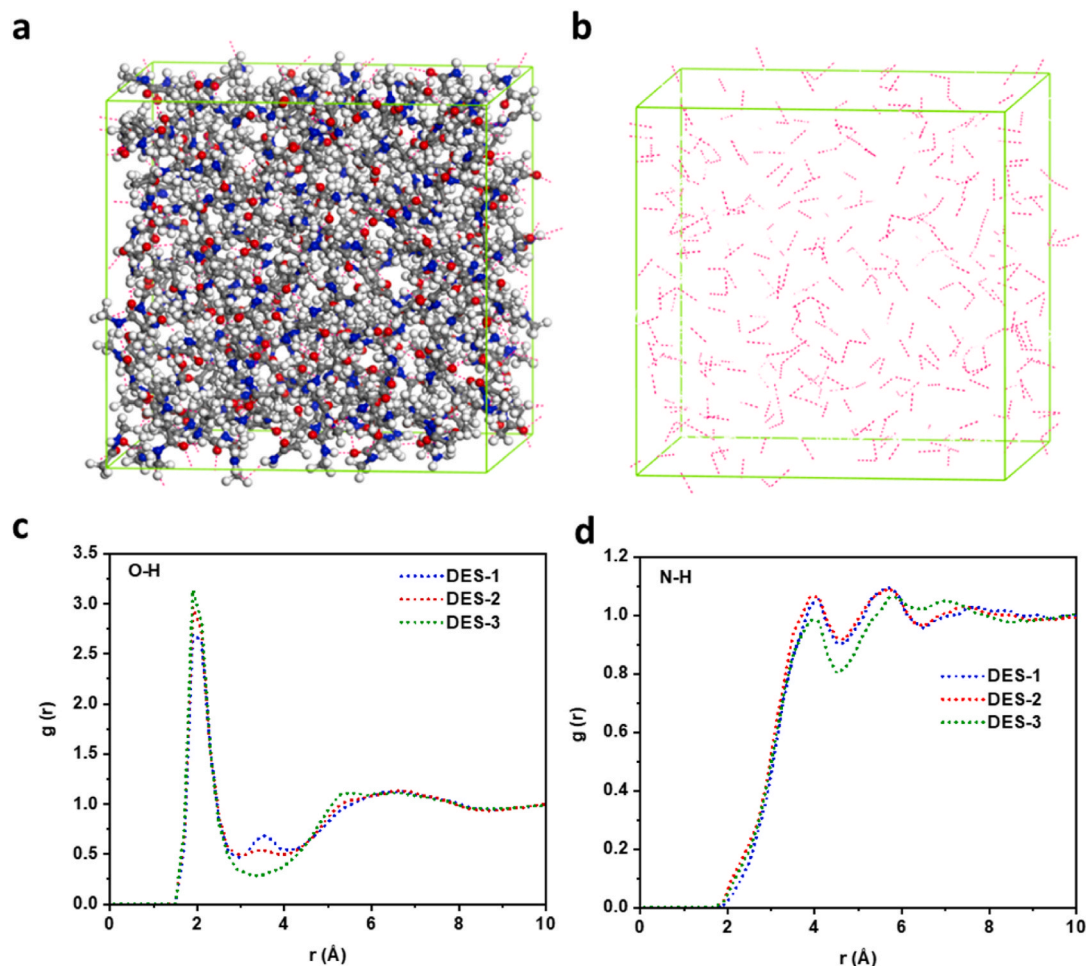


Fig. 2. a) Simulation box of DES-1 shown as an example, b) H-bond formation of DES-1 at the end of the MD simulations, c) O–H and d) N–H radial distribution functions (RDF) of NIDES solutions.

Table 4
Solubility of NIDES solutions, their interaction parameter with PVDF, density and viscosity.

Solvent	δ_D (MPa ^{1/2})	δ_P (MPa ^{1/2})	δ_H (MPa ^{1/2})	PVDF-solvent Interaction parameter, χ	δ (MPa ^{1/2})		ρ (g/cm ³)		μ (cP)	
					Sim. (*)	Cal. (**)	Cal. (**)	Sim.	Exp.	
DES-1	17.02	18.70	16.45	0.66	27.67	30.17	0.98	0.98 ± 0.03	10.6 ± 0.15	
DES-2	16.48	21.96	14.19	0.88	28.86	30.91	1.02	0.99 ± 0.03	7.1 ± 0.25	
DES-3	16.53	20.22	13.53	0.62	28.42	29.41	1.02	0.98 ± 0.03	7.2 ± 0.30	

* Solubility parameters obtained by MD simulation.

** Solubility parameters calculated by the group contribution method.

the formation of spherical structures [19]. L-L phase separation may also result in the formation of finger-like structure when using water-soluble DES. It is therefore expected that both TIPS and NIPS processes will occur simultaneously during the preparation of the PVDF membranes with the proposed NIDES in this study.

3.3. PVDF membrane characteristics

Fig. 4a, b and 4c show the morphological structures of the prepared PVDF membranes with DES-1 using different PVP concentrations (0, 2, and 4 wt%) and a fixed PVDF concentration of 15 wt%. All resulting PVDF membranes exhibit a typical asymmetric structure with a macrovoid sub-layer, an intermediate finger-like structure layer and thin top denser skin layer. By adding PVP to the polymer solution (Fig. 4a and b) larger macro-voids were formed extending through the cross-section of the membrane. The use of a dope solution without PVP resulted in the

formation of a sponge-like structure between finger-like structure (Fig. 4a). The addition of PVP inhibited the formation of this sponge-like structure indicating the fast phase separation. A higher PVP concentration, above 2 wt%, induces the extension of the macro-voids through practically the whole membrane cross-section (Fig. 4c). The addition of PVP thus promotes pore formation and increases pore size due to its high water affinity; the presence of the pore-forming agent induces thermodynamic instability that enforces the formation of two distinct phases and thus increases the rate of solvent/non-solvent exchange during the phase inversion process.

It is to be noted that increasing PVP concentration up to 4 wt% made the casting solution more viscous and thus reduced the solvent/non-solvent exchange rate affecting the structure of the formed membrane [101,102]. This can be explained by two simultaneous effects occur by adding PVP into the polymer matrix. First, adding PVP will create thermodynamic instability, which occur at low PVP concentration.

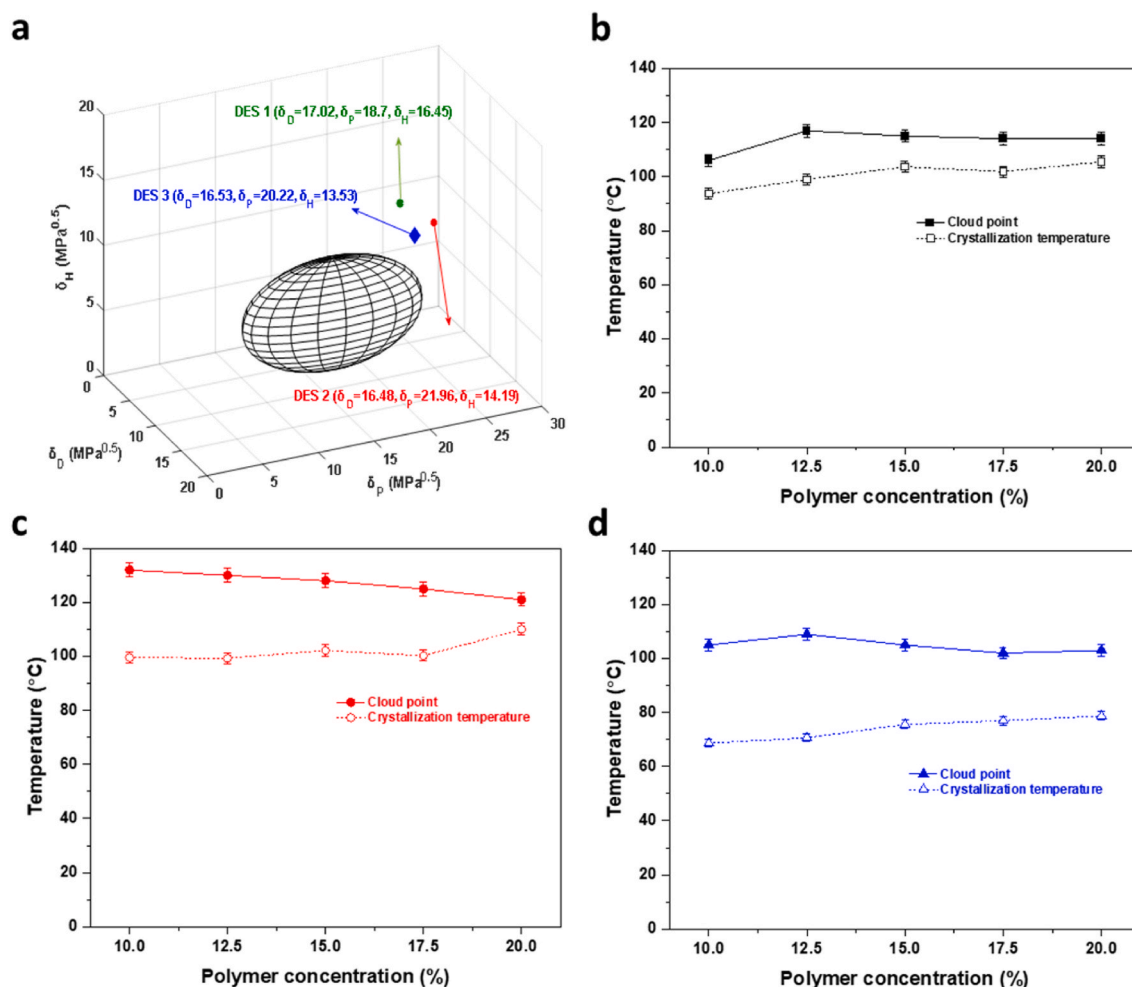


Fig. 3. Solubility sphere of PVDF in Hansen space together with the positions of the three proposed NIDES solvents (a), cloud point and crystallization temperatures of the three PVDF/NIDES systems: b) PVDF/DES-1, c) PVDF/DES-2, and d) PVDF/DES-3.

Secondly, at high PVP concentration, the dope solution viscosity increased thus generated kinetic effect. Therefore, there is a tradeoff between these two factors. Thermodynamic instability increases the rate of phase inversion as it can be seen in 2 wt%. Meanwhile, increasing the PVP concentration higher than 2 wt% increase the impact of the kinetic effect which slow down the rate of phase inversion. Consequently, suppressed the macrovoids formation.

Moreover, the use of high PVP concentrations may be retained within the membrane matrix and cause the formation of a thick skin on the top of the membrane surface. This is consistent with the results of earlier studies [6,101] in which additives were found to promote the formation of denser membrane structures due to their entrapment in pores and macro-void suppression reducing the membrane permeability as consequence [103].

Fig. 4b, d and 4e show different cross-sectional SEM images of the PVDF membranes prepared with different NIDES under the same conditions. The membrane PVDF/2PVP/DES-3 (Fig. 4e) exhibits a bottom thin layer consisting of a sponge-like structure fraction between finger-like structures as can be seen in the corresponding SEM bottom surface of this membranes. The finger-like structures extend to the denser thin top layer. In contrast, the membrane prepared PVDF/2PVP/DES-2 (Fig. 4d) shows only finger-like structure that prolongs to the thin top layer without presence of any sponge-like structure. This is apparent from the SEM image of the bottom surface shown in Fig. 4d. The membrane PVDF/2PVP/DES-1 is formed by a thick bottom layer consisting for big macro-voids, an intermediate thinner finger-like structure

layer and a thin denser top layer. As shown in Table 4, taking into consideration the standard deviation, thermal factors and their effect on viscosity are almost the same for the studied PVDF/DES systems. Moreover, all of the NIDES solvents examined in this work are highly miscible with water. It should be noted that in this case viscosity did not affect significantly the kinetic mass transfer because the membranes were prepared at elevated temperatures. Consequently, the observed differences in membrane morphology are mainly attributed to the differences of solvent/non-solvent exchange rate during NIPS step. The slow solvent/non-solvent diffusion rate during the preparation of the membrane PVDF/2PVP/DES-3 induced the formation of sponge-like structure between finger-like structure and most of the pores at its bottom surface are closed. The appeared macro-voids through the cross-section of the membrane PVDF/2PVP/DES-1 and the absence of finger-like structure indicate the faster solvent/non-solvent demixing rate compared to the membrane PVDF/2PVP/DES-3. As shown in Table 4, DES-2 has the highest χ value of the three NIDES, indicating that DES-2 has the lowest compatibility with PVDF and the highest affinity for the non-solvent (water). Moreover, the membrane PVDF/2PVP/DES-2 exhibits a more distributed and uniform layer of finger-like structure with more open pores on the bottom surface than the membranes PVDF/2PVP/DES-1 and PVDF/2PVP/DES-3. DES-3 has the lowest χ value of the three NIDESs, suggesting that DES-3 has the highest compatibility with PVDF (and low miscibility with water). This reduced the solvent/non-solvent mass exchange rate, suppressing the formation of macrovoids in the support layer.

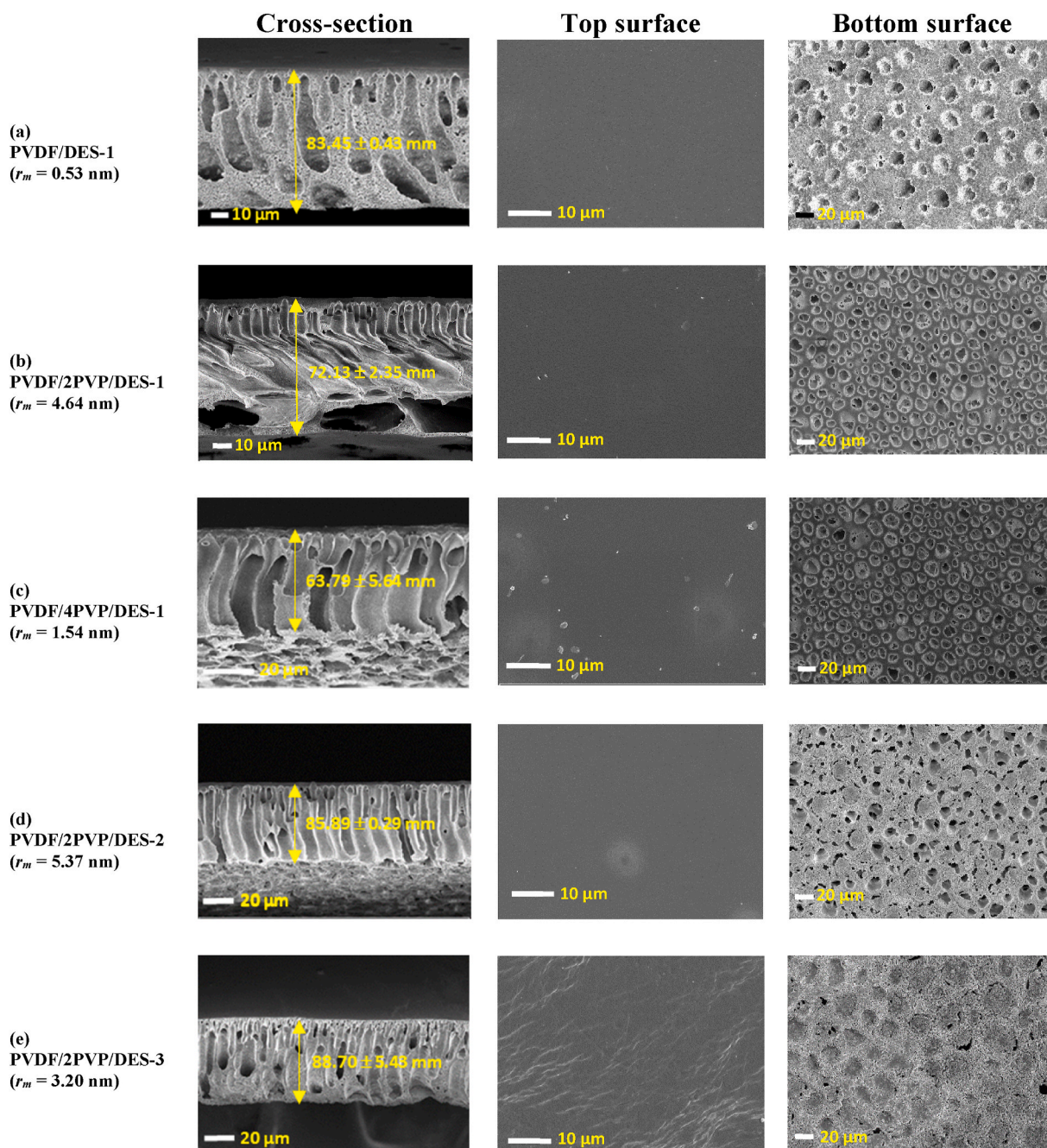


Fig. 4. SEM images showing the cross-section, top surface, and bottom surface of the PVDF membranes prepared with different PVP concentrations and different NIDES.

Fig. 5 shows the tensile strength and elongation at break of the prepared PVDF membranes with different concentrations of PVP and NIDES. For the same solvent, DES-1, both the tensile strength and elongation at break decreased with the increase of PVP concentration. This may be attributed partly to the weaker compatibility of the hydrophobic PVDF with the hydrophilic PVP and the formation of macrovoids at the bottom thick layer of the membrane PVDF/2PVP/DES-1 and their extensions through the whole cross-section of the membrane PVDF/4PVP/DES-3. This result was already observed by Wei et al. [104] when incorporating PVP into the Polyvinyl alcohol (PVA) membranes. It found that PVP additive promoted the formation of finger-like structure and macrovoids, and its excess in the polymer matrix reduced membrane elasticity and ductility.

The three NIDES solvents affected differently the mechanical

properties of the prepared membranes as can be seen in Fig. 5. The membrane PVDF/2PVP/DES-3 exhibited the highest tensile strength and elongation at break, whereas the PVDF/2PVP/DES-2 showed the lowest values. The observed good mechanical properties of the membrane PVDF/2PVP/DES-3 is attributed mainly to the sponge-like structure formed at the bottom layer between finger-like structure (Fig. 4e). In addition, smaller finger-like structure were observed for this membrane compared to PVDF/2PVP/DES-1 and PVDF/2PVP/DES-2 membranes. The low tensile strength and elongation at break of the membrane PVDF/2PVP/DES-2 is due to the finger-like structure cavities that are prolonged through practically the whole cross-section of the membrane.

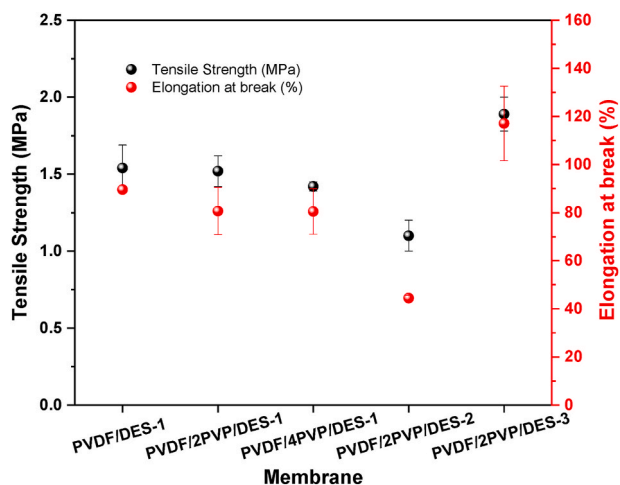


Fig. 5. Tensile strength and elongation at break of PVDF membranes prepared with different PVP concentrations and different NIDES.

3.3.1. Polymorphism of the PVDF membranes

It is well known that PVDF has five distinct polymorph phases known as the α , β , γ , δ , and ϵ forms [105]. PVDF most frequently occurs in the α or β forms while the γ phase is rare [106]. FTIR and XRD were employed to evaluate the crystalline phase of the PVDF membranes prepared in this study with NIDES. The α form of PVDF can be obtained from melt processes or by using solvent or thermal methods, while the β -phase is usually formed by using additives, from solution under highly specific conditions, or by annealing [105].

The FTIR spectra of the prepared PVDF membranes with different

PVP concentrations are shown in Fig. 6a. The transmittance peaks at 532, 615, 764 and 795 cm^{-1} are assigned to the α -phase while those at 840 and 1275 cm^{-1} are assigned to the β -phase for all PVDF membranes. To confirm the polymorphisms of the prepared PVDF membranes, XRD was also carried out and the corresponding spectra are presented in Fig. 6b. The 2θ peaks at 17.4°, 18.1°, 19.6° and 26.5° are assigned to diffraction in the (100), (020), (110) and (021) planes of the α -phase, respectively. A β -phase PVDF peak at 20.26° is also observed for all PVDF membranes indicating that mixtures of α and β phase crystals are present in all membranes prepared in this study, irrespective of the added PVP concentration.

A similar approach was followed to investigate the polymorphism of the PVDF membranes prepared with different NIDES solvents. The FTIR spectra (Fig. 6c) and XRD diffraction data (Fig. 6d) of these membranes show similar mixtures of α and β -phase PVDF irrespective of the NIDES used.

3.4. Water permeability and BSA separation

Fig. 7a and c shows the water permeability and BSA separation factor of the PVDF membranes prepared with different PVP concentrations and NIDES, respectively. All prepared PVDF membranes properties are presented in Table 5. As it was expected, increasing the PVP concentration affected significantly the membrane water permeability, which was increased upon the addition of 2 wt% PVP and then decreased for higher PVP concentration. The observed enhancement of the water permeability with the addition of 2 wt% PVP can be attributed to the formation of larger macro-voids, larger pore size combined (Table 4) with higher overall porosity and hydrophilicity as shown in Fig. 7b. However, the water permeability was decreased when using 4 wt% PVP, this may be attributed to the possible entrapment of PVP molecules

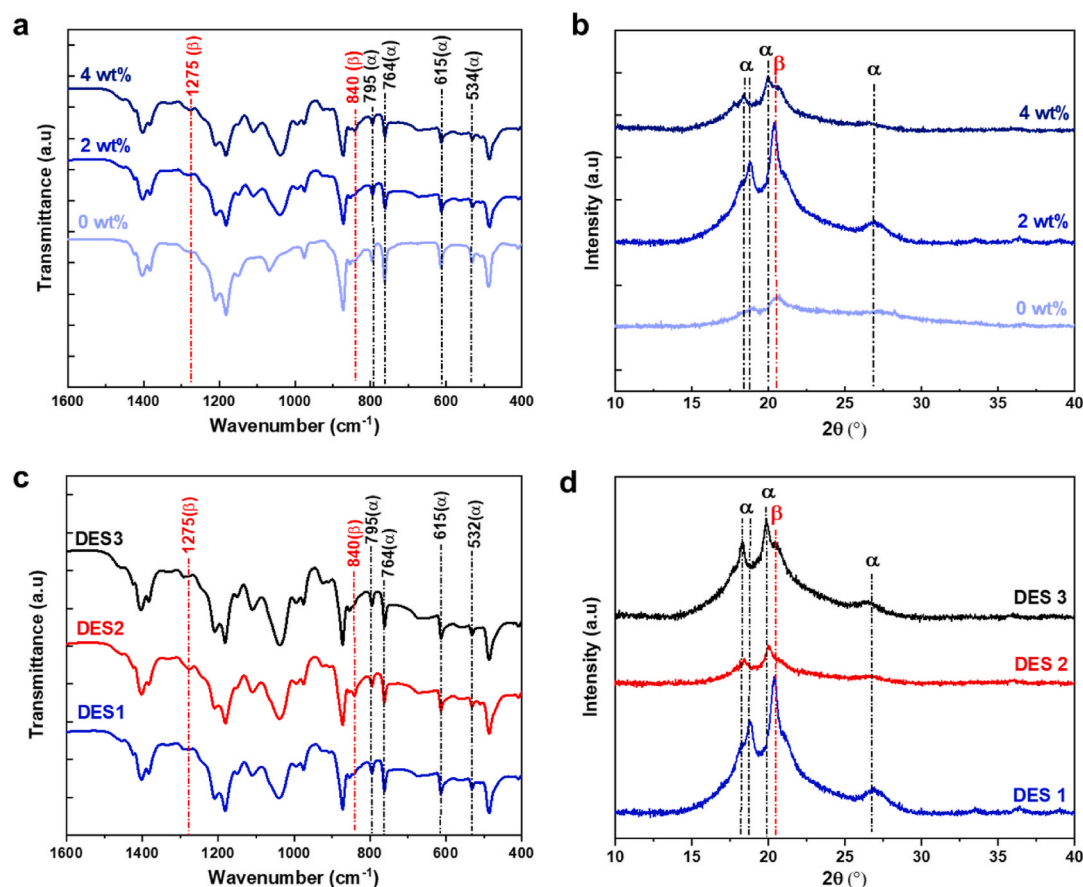


Fig. 6. FTIR (a,c) and XRD (b,d) spectra of PVDF membranes prepared with different PVP concentrations (a,b) and different NIDES (c,d).

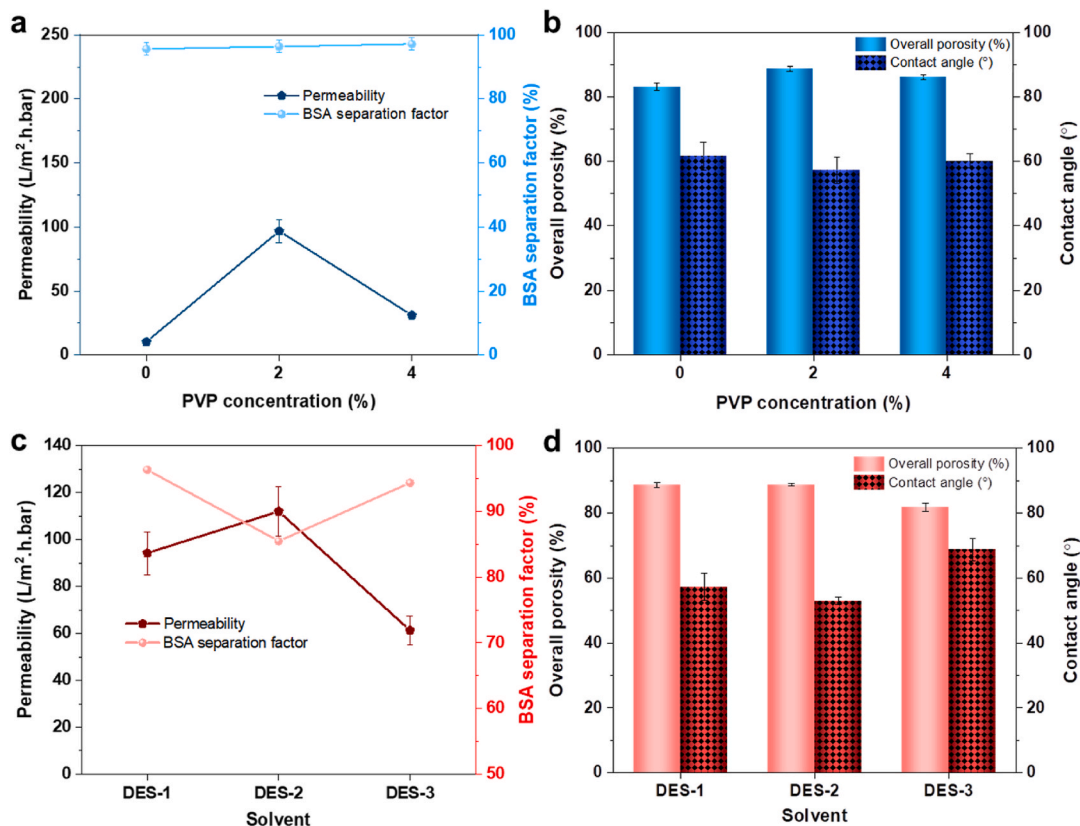


Fig. 7. Pure water permeability and BSA separation factor of the membranes prepared with different PVP concentrations (a), their corresponding overall porosity and water contact angle, and effect of the NIDES solvent on pure water permeability and BSA separation factor (c) and their overall porosity and contact angle (d).

Table 5

Membrane thickness, average pore size and resistance.

Membrane	Thickness (mm)	Average pore size (nm)	Resistance ($\times 10^{11} \text{ m}^{-1}$)
PVDF/0PVP/DES-1	83.45 \pm 0.43	0.53	6.49
PVDF/2PVP/DES-1	72.13 \pm 2.35	4.64	0.69
PVDF/4PVP/DES-1	63.79 \pm 5.64	1.54	2.17
PVDF/2PVP/DES-2	85.89 \pm 0.29	5.37	0.60
PVDF/2PVP/DES-3	88.70 \pm 5.43	3.20	1.10

within the membrane void space causing the reduction of its porosity as can be seen in Fig. 7b [107]. The lower membrane pore size also supporting the result declination of water permeability. In addition, the BSA separation factor was gradually improved with the PVP addition yielding PVDF membranes with good performance, especially the membrane PVDF/2PVP/DES-1.

The effects of the NIDES type on the water permeability and BSA separation was studied considering 2 wt% PVP concentration. As shown in Fig. 7c, the water permeability of membrane PVDF/2PVP/DES-2 (112 L/m² h bar) exceeded that of the membranes PVDF/2PVP/DES-1 and PVDF/2PVP/DES-3 while this last membrane had the lowest pure water permeability (60 L/m² h bar). These results may be attributed to the membrane morphology of the membrane PVDF/2PVP/DES-2, which exhibits an extended finger-like structure through the membrane cross-section, a higher fraction of open pores at the bottom membrane surface, a higher porosity, larger average pore size and a lower water contact angle (i.e. higher hydrophilic character) compared to the other two

membranes. However, this membrane showed a smaller BSA separation factor. In contrast, the membrane PVDF/2PVP/DES-3 exhibited a higher BSA separation factor but a lower water permeability. As shown in the SEM images in Fig. 4e, in contrast to the other membranes, PVDF/2PVP/DES-3 has a sponge bottom layer and smaller finger-like structure with a top denser layer inducing a lower overall porosity as plotted in Fig. 7d. These observations together with the higher hydrophobic character of this membrane (i.e. higher water contact angle (Fig. 7d), and smaller average pore size, with lower membrane resistance (Table 5) result in a lower permeability and the subsequent higher BSA separation factor. Considering the size of BSA in comparison to the average pore size of the membranes, the separation of BSA is most likely based on size exclusion.

Among all prepared PVDF membranes with different NIDES, the membrane PVDF/2PVP/DES-1 exhibited reasonably high water permeability (96.82 L/m² h bar) with a good BSA separation factor of 96.32%. Its performance was compared to previously reported membranes as shown in Table 6. It was found that this membrane achieved high BSA separation factor compared to most reported PVDF membranes in the literature with a reasonably high permeate flux and acceptable mechanical stability suggesting that the NIDES solvents proposed in this study offer an inexpensive, scalable solvents with low toxicity for membrane preparation. Unfortunately, many published papers related to PVDF membrane did not report the mechanical strength of their fabricated membranes. Yet, it can be concluded from the reported data the tensile strength of PVDF membrane is often in the range of 1–5 MPa [108].

3.5. Toxicity and cost

Table 7 presents the solvent classification according to EU-regulation no. 1272/2008 [134] and comparison with the most popular solvents used in membrane preparation [135] NMA is identified as

Table 6
Comparison of the pure water permeate flux, BSA rejection factor and mechanical properties achieved in this study and in previous works for PVDF membranes.

Polymer	Additives	Solvent	Membrane preparation	Pure water Flux (L/m ² .h)	BSA separation factor (%)	Tensile strength (MPa)	Elongation at break (%)	Operating pressure (bar)	Ref.
PVDF	GO	DMAC	Flat sheet	457.9	91.1	5.4	60	1 bar	[109]
PVDF	^a OMWCNT-GO/PVP	DMAC	Flat sheet	203.0	82.0	1.75	6.5	1 bar	[110]
PVDF	^b GO	DMAC	Flat sheet	467.8	67.6			1 bar	[111]
PVDF	^c AA	DMAC	Flat sheet	145.0	83.0			1 bar	[112]
PVDF	rGO/TiO ₂		Flat sheet	≈225	98.5			3 bar	[113]
PVDF	γ-Alumina	NMP	Flat sheet	134.4	93.5	1.92	97.5	1 bar	[114]
PVDF	TiO ₂	NMP	Flat sheet	237	70.6	11 N	41.2	1 bar	[115]
PVDF (commercial)			Flat sheet	1243.4	55.9			1 bar	[116]
PVDF	PEO-PPO-PEO	DMAC	Flat sheet	1136	64			1 bar	[117]
PVDF	PEO-PPO-PEO/Oxalic acid	DMAC	Flat sheet	2271	55.6			1 bar	[118]
PVDF	Chitosan	DMF	Electrospinning	70.5	98.9			2 bar	[118]
PVDF	Crosslinked and modified by glutaraldehyde (GA)and terephthaloyl chloride (TPC) Citric acid monohydrate	DMF	Free standing membrane	318.31				Gravity	[119]
PVDF	ZrO ₂ solid superacid shell/void/TiO ₂ core particles	DMAC	Flat sheet membrane	640		3.05		1 bar	[120]
PVDF			Hollow fiber membrane	590	82%	4.24	101	1 bar	[121]
PVDF	TiO ₂ /PVP	DMAC	Hollow fiber membrane	72.2	95	2.18	3	1 bar	[122]
PVDF	TiO ₂	DMAC	Hollow fiber membrane	70.48				1 bar	[123]
PVDF	Amphiphilic TBC	NMP	Flat sheet membrane	FRR – 67- 68	60.5			2 bar	[124]
PVDF	TiO ₂	DMAC	Hollow fiber	82.5				0.5 bar	[125]
PVDF	Hexaphosphate/PVP/nano-sized Al ₂ O ₃ particles	DMAC	Tubular	138.53					[126]
PVDF-PANI			Flat sheet	3000				0.1 bar	[127]
PVDF	KH550–TiO ₂		Flat sheet	382				0.09 MPa	[128]
PVDF	g-PVP		Flat sheet	320				0.3 MPa	[129]
PVDF (commercial)	Chitosan-SiO ₂		Flat sheet					0.03 MPa	[130]
PVDF	PEO	DMF	Nanofiber	1172		20.35	380	0.2 bar	[131]
PVDF	Citric acid monohydrate	DMF	Free standing membrane	318					[119]
PVDF/ Polycarbonate	PVP	DMAC	Flat sheet	22.11				60–80 kPa	[132]
PVDF		DMAC	Flat sheet	92.74				1 bar	[133]
PVDF	PVP	DES-1	Flat sheet	96.82	96.32	1.25	97	1	This study
PVDF	PVP	DES-2	Flat sheet	112	85	0.7	70	1	This study

Table 7
Hazard identification and toxicology information of the common solvents and NIDES.

Solvent (Price €/L)	Hazard identification	Toxicology information	Biodegradability
NMA (50–60 €/L)	H360D – Reproductive toxicity 1B	Mild skin irritation Not carcinogenic	70% readily biodegradable
AA (103 €/L)	Carcinogenic category 2, H351	IARC: 2B possibly carcinogenic to human	–
NMU (112 €/L)	–	Not carcinogenic	–
N,N'-DMU (57 €/L)	Not a hazardous substance or mixture	No skin or eye irritation Not carcinogenic	90–100% Readily biodegradable
NMP (130–150 €/L)	Cause skin irritation Cause eye irritation May cause respiratory irritation May damage the unborn child (Damage fetus)	Possible to damage the fetus	–
DMF (130–200 €/L)	Flammable liquid and vapor Harmful in contact with skin	Toxic if inhaled Mutations in mammalian somatic cells	–
DMAC (110 €/L)	Cause serious eye irritation H319 –Cause eye irritation Harmful in contact with skin H360D –May damage unborn child	Germ cell mutagenicity Toxic if inhaled Presumed human reproductive toxicant	–

*Prices of the solvents are taken from Sigma-Aldrich and TCI chemicals Sweden websites. <https://www.sigmaaldrich.com/SE/en> and <https://www.tcichemicals.com/SE/en>.

**Hazard, toxicology and biodegradability information are taken from Regulation (EC) [134], MSDS Europe [136] and Globally Harmonized System of Classification and Labelling of Chemicals (GHS) [137].

non-carcinogenic to human with good biodegradability, even though it has possibility to cause mild skin irritation and reproductive toxicity. NMU and N,N'-DMU both are classified as non-carcinogenic chemicals that are safe to use since no hazards or toxicity has been documented in EU-regulation. Furthermore, N,N'-DMU is 90% rapidly biodegradable, which easily breaking down into benign degradation products that do not remain in the environment. Using AA in the NIDES system should be avoided or minimized due to the carcinogenic effect of AA (30 wt% in this study). NMU-NMA (DES-2) on the other hand is an interesting candidate as it presents low toxicity with biodegradable properties.

All components of the NIDES solvents used in this work have relatively low material costs, ranging from 50 to 70 €/L (calculated based on the proposed composition ratio of NIDES). Therefore, in addition to being less toxic than traditional solvents, the presented NIDESs are also less costly; DMAc and NMP currently cost around 110 €/L and 130–150 €/L, respectively. They are also cheaper than alternative greener solvents such as Dimethylisobutylacetate (112 €/L) and Cyrene™ (155 €/L). Thanks to one-step, simple synthesizing process without producing any byproduct, NIDES offer important advantages in large-scale production.

4. Conclusions

A new family of non-ionic deep eutectic solvents (NIDES) are proposed in this study for PVDF membrane preparation. These were synthesized as NMA-AA (DES-1), NMA-NMU (DES-2), and NMA-N,N'-DMU (DES-3). To find optimal conditions for PVDF membrane formation, the effect of different concentrations of the additive PVP on membrane

morphology and performance was investigated using PVDF polymer DES-1. It was found that adding PVP to the casting solution induced the formation of large macro-voids and finger-like structure that extended through the whole membrane cross-section, an enhanced hydrophilic character, overall porosity, water permeability and BSA separation factor. A PVP content of 2 wt% was found to be optimal with respect to water permeability while maintaining acceptable BSA separation factor. The effect of varying the NIDES type, was investigated using a fixed PVP concentration of 2 wt%. The membrane prepared with DES 1 (PVDF/2PVP/DES-1) was found to have the optimal water permeability and BSA removal performance comparable to that of other PVDF membranes prepared with conventional and toxic solvents. The good membrane performance achieved using the proposed NIDES in this study together with their low cost and toxicity suggest their attractive alternatives to conventional toxic solvents for membrane fabrication. The cost, toxicity and biodegradability of DES depend on the selected type of the hydrogen donor and hydrogen acceptor. By choosing suitable types of hydrogen donor and hydrogen acceptor one can synthesize competitive DES for membrane fabrication.

Author statement

Norafiqah Ismail: Conceptualization, Data curation, membrane formation, membrane characterization, Writing - original Draft and revision. Jun Pan: Membrane characterization, Writing - original Draft and revision. Mahmoud Rahmati: Simulation, Writing - original Draft and revision. Qian Wang: Membrane characterization, Writing - original Draft and revision. Denis Bouyer: Conceptualization, Supervision, Writing - original Draft and revision. Mohamed Khayet: Conceptualization, Supervision, editing - original Draft and revision. Zhaoliang Cui: Funding acquisition, Conceptualization, Supervision, editing - original Draft and revision. Naser Tavajohi: Funding acquisition, Conceptualization, Supervision, editing - original Draft and revision, Project administration.

Declaration of competing interest

The authors declare that they have no known competing financial interests or personal relationships that could have appeared to influence the work reported in this paper.

Acknowledgements

The authors would like to express their appreciation for the financial support of Kempestiftelserna (SMK-1850) and Bio4energy program (B4E3-TM-1-01). The authors would like to express their appreciation for the financial support of the National Natural Science Foundation of China (22078146), the Natural Science Foundation of Jiangsu Province (BK20200091), the Jiangsu Province Department of Human Resources and Social Security (JNHB-036), the Materials-Oriented Chemical Engineering State Key Laboratory Program (KL19-04) and the Priority Academic Program Development of Jiangsu Higher Education Institution (PAPD).

Appendix A. Supplementary data

Supplementary data to this article can be found online at <https://doi.org/10.1016/j.memsci.2021.120238>.

References

- [1] S. Loeb, S. Sourirajan, Sea water demineralization by means of an osmotic membrane, in: *Saline Water Conversion—II*, American Chemical Society, 1963, pp. 117–132.
- [2] Z. Cui, N.T. Hassankiadeh, S.Y. Lee, J.M. Lee, K.T. Woo, A. Sanguineti, V. Arcella, Y.M. Lee, E. Drioli, Poly(vinylidene fluoride) membrane preparation with an

- environmental diluent via thermally induced phase separation, *J. Membr. Sci.* 444 (2013) 223–236.
- [3] M. Razali, J.F. Kim, M. Attfield, P.M. Budd, E. Drioli, Y.M. Lee, G. Szekely, Sustainable wastewater treatment and recycling in membrane manufacturing, *Green Chem.* 17 (2015) 5196–5205.
- [4] T. Marino, F. Galiano, S. Simone, A. Figoli, DMSO EVOL™ as novel non-toxic solvent for polyethersulfone membrane preparation, *Environ. Sci. Pollut. Control Ser.* 26 (2019) 14774–14785.
- [5] A. Figoli, T. Marino, S. Simone, E. Di Nicolò, X.M. Li, T. He, S. Tornaghi, E. Drioli, Towards non-toxic solvents for membrane preparation: a review, *Green Chem.* 16 (2014) 4034–4059.
- [6] N.T. Hassankiadeh, Z. Cui, J.H. Kim, D.W. Shin, S.Y. Lee, A. Sanguineti, V. Arcella, Y.M. Lee, E. Drioli, Microporous poly(vinylidene fluoride) hollow fiber membranes fabricated with PolarClean as water-soluble green diluent and additives, *J. Membr. Sci.* 479 (2015) 204–212.
- [7] T. Marino, F. Galiano, A. Molino, A. Figoli, New frontiers in sustainable membrane preparation: Cyrene™ as green bioderived solvent, *J. Membr. Sci.* 580 (2019) 224–234.
- [8] S. Khandelwal, Y.K. Tailor, M. Kumar, Deep eutectic solvents (DESs) as eco-friendly and sustainable solvent/catalyst systems in organic transformations, *J. Mol. Liq.* 215 (2016) 345–386.
- [9] T.P. Thuy Pham, C.-W. Cho, Y.-S. Yun, Environmental fate and toxicity of ionic liquids: a review, *Water Res.* 44 (2010) 352–372.
- [10] M. Cvjetko Bubalo, K. Radošević, I. Radojević Redovniković, J. Halambek, V. Gaurina Srček, A brief overview of the potential environmental hazards of ionic liquids, *Ecotoxicol. Environ. Saf.* 99 (2014) 1–12.
- [11] E.L. Smith, A.P. Abbott, K.S. Ryder, Deep eutectic solvents (DESs) and their applications, *Chem. Rev.* 114 (2014) 11060–11082.
- [12] Y. Liu, J.B. Friesen, J.B. McAlpine, D.C. Lankin, S.-N. Chen, G.F. Pauli, Natural deep eutectic solvents: properties, applications, and perspectives, *J. Nat. Prod.* 81 (2018) 679–690.
- [13] N. Ndizeye, S. Suriyanarayanan, I.A. Nicholls, Polymer synthesis in non-ionic deep eutectic solvents, *Polym. Chem.* 10 (2019) 5289–5295.
- [14] B. Jiang, N. Zhang, B. Wang, N. Yang, Z. Huang, H. Yang, Z. Shu, Deep eutectic solvent as novel additive for PES membrane with improved performance, *Separ. Purif. Technol.* 194 (2018) 239–248.
- [15] B. Jiang, N. Zhang, L. Zhang, Y. Sun, Z. Huang, B. Wang, H. Dou, H. Guan, Enhanced separation performance of PES ultrafiltration membranes by imidazole-based deep eutectic solvents as novel functional additives, *J. Membr. Sci.* 564 (2018) 247–258.
- [16] V. Vatanpour, A. Dehqan, A.R. Harifi-Mood, Ethaline deep eutectic solvent as a hydrophilic additive in modification of polyethersulfone membrane for antifouling and separation improvement, *J. Membr. Sci.* 614 (2020) 118528.
- [17] Z. Cui, E. Drioli, Y.M. Lee, Recent progress in fluoropolymers for membranes, *Prog. Polym. Sci.* 39 (2014) 164–198.
- [18] D.R. Lloyd, K.E. Kinzer, H.S. Tseng, Microporous membrane formation via thermally induced phase separation. I. Solid-liquid phase separation, *J. Membr. Sci.* 52 (1990) 239–261.
- [19] D.R. Lloyd, S.S. Kim, K.E. Kinzer, Microporous membrane formation via thermally-induced phase separation. II. Liquid-liquid phase separation, *J. Membr. Sci.* 64 (1991) 1–11.
- [20] S.S. Kim, D.R. Lloyd, Microporous membrane formation via thermally-induced phase separation. III. Effect of thermodynamic interactions on the structure of isotactic polypropylene membranes, *J. Membr. Sci.* 64 (1991) 13–29.
- [21] G.B.A. Lim, S.S. Kim, Q. Ye, Y.F. Wang, D.R. Lloyd, Microporous membrane formation via thermally-induced phase separation. IV. Effect of isotactic polypropylene crystallization kinetics on membrane structure, *J. Membr. Sci.* 64 (1991) 31–40.
- [22] S.S. Kim, G.B.A. Lim, A.A. Alwattari, Y.F. Wang, D.R. Lloyd, Microporous membrane formation via thermally-induced phase separation. V. Effect of diluent mobility and crystallization on the structure of isotactic polypropylene membranes, *J. Membr. Sci.* 64 (1991) 41–53.
- [23] A.A. Alwattari, D.R. Lloyd, Microporous membrane formation via thermally-induced phase separation. VI. Effect of diluent morphology and relative crystallization kinetics on polypropylene membrane structure, *J. Membr. Sci.* 64 (1991) 55–67.
- [24] K.S. McGuire, D.R. Lloyd, G.B.A. Lim, Microporous membrane formation via thermally-induced phase separation. VII. Effect of dilution, cooling rate, and nucleating agent addition on morphology, *J. Membr. Sci.* 79 (1993) 27–34.
- [25] A. Laxminarayan, K.S. McGuire, S.S. Kim, D.R. Lloyd, Effect of initial composition, phase separation temperature and polymer crystallization on the formation of microcellular structures via thermally induced phase separation, *Polymer* 35 (1994) 3060–3068.
- [26] K.S. McGuire, A. Laxminarayan, D.R. Lloyd, A simple method of extrapolating the coexistence curve and predicting the melting point depression curve from cloud point data for polymer-diluent systems, *Polymer* 35 (1994) 4404–4407.
- [27] K.S. McGuire, A. Laxminarayan, D.S. Martula, D.R. Lloyd, Kinetics of droplet growth in liquid-liquid phase separation of polymer-diluent systems: model development, *J. Colloid Interface Sci.* 182 (1996) 46–58.
- [28] H. Matsuyama, M. Yuasa, Y. Kitamura, M. Teramoto, D.R. Lloyd, Structure control of anisotropic and asymmetric polypropylene membrane prepared by thermally induced phase separation, *J. Membr. Sci.* 179 (2000) 91–100.
- [29] W. Yave, R. Quijada, M. Ulbricht, R. Benavente, Syndiotactic polypropylene as potential material for the preparation of porous membranes via thermally induced phase separation (TIPS) process, *Polymer* 46 (2005) 11582–11590.
- [30] W. Yave, R. Quijada, D. Serafini, D.R. Lloyd, Effect of the polypropylene type on polymer-diluent phase diagrams and membrane structure in membranes formed via the TIPS process: Part II. Syndiotactic and isotactic polypropylenes produced using metallocene catalysts, *J. Membr. Sci.* 263 (2005) 154–159.
- [31] M.R. Caplan, C.-Y. Chiang, D.R. Lloyd, L.Y. Yen, Formation of microporous Teflon® PFA membranes via thermally induced phase separation, *J. Membr. Sci.* 130 (1997) 219–237.
- [32] H. Matsuyama, H. Okafuji, T. Maki, M. Teramoto, N. Kubota, Preparation of polyethylene hollow fiber membrane via thermally induced phase separation, *J. Membr. Sci.* 223 (2003) 119–126.
- [33] Z. Yang, P. Li, L. Xie, Z. Wang, S.-C. Wang, Preparation of iPP hollow-fiber microporous membranes via thermally induced phase separation with co-solvents of DBP and DOP, *Desalination* 192 (2006) 168–181.
- [34] Z. Yang, P. Li, H. Chang, S. Wang, Effect of diluent on the morphology and performance of IPP hollow fiber microporous membrane via thermally induced phase separation 1 1 Supported by the national natural science foundation of China (No.20236030), *Chin. J. Chem. Eng.* 14 (2006) 394–397.
- [35] M. Gu, J. Zhang, X. Wang, H. Tao, L. Ge, Formation of poly(vinylidene fluoride) (PVDF) membranes via thermally induced phase separation, *Desalination* 192 (2006) 160–167.
- [36] M. Gu, J. Zhang, X. Wang, W. Ma, Crystallization behavior of PVDF in PVDF-DMP system via thermally induced phase separation, *J. Appl. Polym. Sci.* 102 (2006) 3714–3719.
- [37] Y. Su, C. Chen, Y. Li, J. Li, Preparation of PVDF membranes via TIPS method: the effect of mixed diluents on membrane structure and mechanical property, *J. Macromol. Sci., Part A* 44 (2007) 305–313.
- [38] Y. Su, C. Chen, Y. Li, J. Li, PVDF membrane formation via thermally induced phase separation, *J. Macromol. Sci., Part A* 44 (2007) 99–104.
- [39] G.-I. Ji, L.-p. Zhu, B.-k. Zhu, Y.-y. Xu, Effect of diluents on crystallization of poly(vinylidene fluoride) and phase separated structure in a ternary system via thermally induced phase separation, *Chin. J. Polym. Sci.* 26 (2008) 291–298.
- [40] G.-L. Ji, L.-P. Zhu, B.-K. Zhu, C.-F. Zhang, Y.-Y. Xu, Structure formation and characterization of PVDF hollow fiber membrane prepared via TIPS with diluent mixture, *J. Membr. Sci.* 319 (2008) 264–270.
- [41] J. Yang, D.W. Li, Y.K. Lin, X.L. Wang, F. Tian, Z. Wang, Formation of a bicontinuous structure membrane of polyvinylidene fluoride in diphenyl ketone diluent via thermally induced phase separation, *J. Appl. Polym. Sci.* 110 (2008) 341–347.
- [42] X. Han, H. Ding, L. Wang, C. Xiao, Effects of nucleating agents on the porous structure of polyphenylene sulfide via thermally induced phase separation, *J. Appl. Polym. Sci.* 107 (2008) 2475–2479.
- [43] X. Li, Y. Wang, X. Lu, C. Xiao, Morphology changes of polyvinylidene fluoride membrane under different phase separation mechanisms, *J. Membr. Sci.* 320 (2008) 477–482.
- [44] X. Lu, X. Li, Preparation of polyvinylidene fluoride membrane via a thermally induced phase separation using a mixed diluent, *J. Appl. Polym. Sci.* 114 (2009) 1213–1219.
- [45] Y.-H. Lin, P.-C. Lee, T.-P. Chang, Practical expert diagnosis model based on the grey relational analysis technique, *Expert Syst. Appl.* 36 (2009) 1523–1528.
- [46] H.-h. Lin, Y.-h. Tang, T.-y. Liu, H. Matsuyama, X.-l. Wang, Understanding the thermally induced phase separation process via a Maxwell-Stefan model, *J. Membr. Sci.* 507 (2016) 143–153.
- [47] Y.K. Lin, G. Chen, J. Yang, X.L. Wang, Formation of isotactic polypropylene membranes with bicontinuous structure and good strength via thermally induced phase separation method, *Desalination* 236 (2009) 8–15.
- [48] Y. Tang, Y. Lin, W. Ma, Y. Tian, J. Yang, X. Wang, Preparation of microporous PVDF membrane via tips method using binary diluent of DPK and PG, *J. Appl. Polym. Sci.* 118 (2010) 3518–3523.
- [49] W. Ma, S. Chen, J. Zhang, X. Wang, Kinetics of thermally induced phase separation in the PVDF blend/methyl salicylate system and its effect on membrane structures, *J. Macromol. Sci., Part B* 50 (2010) 1–15.
- [50] S. Rajabzadeh, C. Liang, Y. Ohmukai, T. Maruyama, H. Matsuyama, Effect of additives on the morphology and properties of poly(vinylidene fluoride) blend hollow fiber membrane prepared by the thermally induced phase separation method, *J. Membr. Sci.* 423–424 (2012) 189–194.
- [51] H.-P. Xu, W.-Z. Lang, X. Zhang, Y.-J. Guo, Preparation and characterizations of charged PVDF membranes via composite thermally induced phase separation (C-TIPS) method, *J. Ind. Eng. Chem.* 21 (2015) 1005–1013.
- [52] J. Pan, C. Xiao, Q. Huang, C. Wang, H. Liu, Fabrication and properties of poly(ethylene chlorotrifluoroethylene) membranes via thermally induced phase separation (TIPS), *RSC Adv.* 5 (2015) 45249–45257.
- [53] A. Bottino, G. Camera-Roda, G. Capannelli, S. Munari, The formation of microporous polyvinylidene difluoride membranes by phase separation, *J. Membr. Sci.* 57 (1991) 1–20.
- [54] M.R.M. Abed, S.C. Kumbharkar, A.M. Groth, K. Li, Ultrafiltration PVDF hollow fibre membranes with interconnected bicontinuous structures produced via a single-step phase inversion technique, *J. Membr. Sci.* 407–408 (2012) 145–154.
- [55] H. Sun, K.B. Rhee, T. Kitano, S.I. Mah, HDPE hollow-fiber membrane via thermally induced phase separation. II. Factors affecting the water permeability of the membrane, *J. Appl. Polym. Sci.* 75 (2000) 1235–1242.
- [56] M. Shang, H. Matsuyama, M. Teramoto, D.R. Lloyd, N. Kubota, Preparation and membrane performance of poly(ethylene-co-vinyl alcohol) hollow fiber membrane via thermally induced phase separation, *Polymer* 44 (2003) 7441–7447.

- [57] X. Fu, H. Matsuyama, M. Teramoto, H. Nagai, Preparation of hydrophilic poly(vinyl butyral) hollow fiber membrane via thermally induced phase separation, *Separ. Purif. Technol.* 45 (2005) 200–207.
- [58] X. Fu, H. Matsuyama, M. Teramoto, H. Nagai, Preparation of polymer blend hollow fiber membrane via thermally induced phase separation, *Separ. Purif. Technol.* 52 (2006) 363–371.
- [59] Y.-R. Qiu, N.A. Rahman, H. Matsuyama, Preparation of hydrophilic poly(vinyl butyral)/Pluronic F127 blend hollow fiber membrane via thermally induced phase separation, *Separ. Purif. Technol.* 61 (2008) 1–8.
- [60] Y.-R. Qiu, H. Matsuyama, G.-Y. Gao, Y.-W. Ou, C. Miao, Effects of diluent molecular weight on the performance of hydrophilic poly(vinyl butyral)/Pluronic F127 blend hollow fiber membrane via thermally induced phase separation, *J. Membr. Sci.* 338 (2009) 128–134.
- [61] Q. Wang, Z. Wang, Z. Wu, Effects of solvent compositions on physicochemical properties and anti-fouling ability of PVDF microfiltration membranes for wastewater treatment, *Desalination* 297 (2012) 79–86.
- [62] D.-J. Lin, C.-L. Chang, C.-K. Lee, L.-P. Cheng, Preparation and characterization of microporous PVDF/PMMA composite membranes by phase inversion in water/DMSO solutions, *Eur. Polym. J.* 42 (2006) 2407–2418.
- [63] Z. Song, M. Xing, J. Zhang, B. Li, S. Wang, Determination of phase diagram of a ternary PVDF/ γ -BL/DOP system in TIPS process and its application in preparing hollow fiber membranes for membrane distillation, *Separ. Purif. Technol.* 90 (2012) 221–230.
- [64] S. Bey, A. Criscuoli, S. Simone, A. Figoli, M. Benamor, E. Drioli, Hydrophilic PEEK-WC hollow fibre membrane contactors for chromium (VI) removal, *Desalination* 283 (2011) 16–24.
- [65] M. Liu, Z.-I. Xu, D.-g. Chen, Y.-m. Wei, Preparation and characterization of microporous PVDF membrane by thermally induced phase separation from a ternary polymer/solvent/non-solvent system, *Desalination Water Treat.* 17 (2010) 183–192.
- [66] H.J.M.D. Mullette, *Halar Membranes*, 2005.
- [67] N. Li, C. Xiao, S. Mei, S. Zhang, The multi-pore-structure of polymer-silicon hollow fiber membranes fabricated via thermally induced phase separation combining with stretching, *Desalination* 274 (2011) 284–291.
- [68] S. Rajabzadeh, T. Maruyama, Y. Ohmukai, T. Sotani, H. Matsuyama, Preparation of PVDF/PMMA blend hollow fiber membrane via thermally induced phase separation (TIPS) method, *Separ. Purif. Technol.* 66 (2009) 76–83.
- [69] S. Rajabzadeh, M. Teramoto, M.H. Al-Marzouqi, E. Kamio, Y. Ohmukai, T. Maruyama, H. Matsuyama, Experimental and theoretical study on propylene absorption by using PVDF hollow fiber membrane contactors with various membrane structures, *J. Membr. Sci.* 346 (2010) 86–97.
- [70] N. Ghasem, M. Al-Marzouqi, A. Duaidar, Effect of quenching temperature on the performance of poly(vinylidene fluoride) microporous hollow fiber membranes fabricated via thermally induced phase separation technique on the removal of CO₂ from CO₂-gas mixture, *Int. J. Greenh. Gas Control* 5 (2011) 1550–1558.
- [71] N. Ghasem, M. Al-Marzouqi, A. Duaidar, Effect of PVDF concentration on the morphology and performance of hollow fiber membrane employed as gas-liquid membrane contactor for CO₂ absorption, *Separ. Purif. Technol.* 98 (2012) 174–185.
- [72] N. Ghasem, M. Al-Marzouqi, N. Abdul Rahim, Effect of polymer extrusion temperature on poly(vinylidene fluoride) hollow fiber membranes: properties and performance used as gas-liquid membrane contactor for CO₂ absorption, *Separ. Purif. Technol.* 99 (2012) 91–103.
- [73] E. Drioli, S. Santoro, S. Simone, G. Barbieri, A. Brunetti, F. Macedonio, A. Figoli, ECTFE membrane preparation for recovery of humidified gas streams using membrane condenser, *React. Funct. Polym.* 79 (2014) 1–7.
- [74] X.Y. Fu, T. Sotani, H. Matsuyama, Effect of membrane preparation method on the outer surface roughness of cellulose acetate butyrate hollow fiber membrane, *Desalination* 233 (2008) 10–18.
- [75] T. Shibutani, T. Kitaura, Y. Ohmukai, T. Maruyama, S. Nakatsuka, T. Watabe, H. Matsuyama, Membrane fouling properties of hollow fiber membranes prepared from cellulose acetate derivatives, *J. Membr. Sci.* 376 (2011) 102–109.
- [76] Z. Cui, N.T. Hassankiadeh, S.Y. Lee, K.T. Woo, J.M. Lee, A. Sanguineti, V. Arcella, Y.M. Lee, E. Drioli, Tailoring novel fibrillar morphologies in poly(vinylidene fluoride) membranes using a low toxic triethylene glycol diacetate (TEGDA) diluent, *J. Membr. Sci.* 473 (2015) 128–136.
- [77] T. Marino, E. Blasi, S. Tornaghi, E. Di Nicolò, A. Figoli, Polyethersulfone membranes prepared with Rhodiasolv®/Polarclean as water soluble green solvent, *J. Membr. Sci.* 549 (2018) 192–204.
- [78] T. Marino, F. Russo, A. Criscuoli, A. Figoli, TamiSolve® NxG as novel solvent for polymeric membrane preparation, *J. Membr. Sci.* 542 (2017) 418–429.
- [79] Z. Cui, Y. Cheng, K. Xu, J. Yue, Y. Zhou, X. Li, Q. Wang, S.-P. Sun, Y. Wang, X. Wang, Z. Wang, Wide liquid-liquid phase separation region enhancing tensile strength of poly(vinylidene fluoride) membranes via TIPS method with a new diluent, *Polymer* 141 (2018) 46–53.
- [80] F. Russo, F. Galiano, F. Pedace, F. Aricò, A. Figoli, Dimethyl isosorbide as a green solvent for sustainable ultrafiltration and microfiltration membrane preparation, *ACS Sustain. Chem. Eng.* 8 (2020) 659–668.
- [81] G. Liu, J. Pan, X. Xu, Z. Wang, Z. Cui, Preparation of ECTFE porous membrane with a green diluent TOTM and performance in VMD process, *J. Membr. Sci.* 612 (2020) 118375.
- [82] D.Y. Xing, N. Peng, T.-S. Chung, formation of cellulose acetate membranes via phase inversion using ionic liquid, [BMIM]SCN, as the solvent, *Ind. Eng. Chem. Res.* 49 (2010) 8761–8769.
- [83] D.Y. Xing, S.Y. Chan, T.-S. Chung, The ionic liquid [EMIM]OAc as a solvent to fabricate stable polybenzimidazole membranes for organic solvent nanofiltration, *Green Chem.* 16 (2014) 1383–1392.
- [84] D.S. Lakshmi, T. Cundari, E. Furià, A. Tagarelli, G. Fiorani, M. Carraro, A. Figoli, Preparation of polymeric membranes and microcapsules using an ionic liquid as morphology control additive, *Macromol. Symp.* 357 (2015) 159–167.
- [85] X. Wang, X. Li, J. Yue, Y. Cheng, K. Xu, Q. Wang, F. Fan, Z. Wang, Z. Cui, Fabrication of poly(vinylidene fluoride) membrane via thermally induced phase separation using ionic liquid as green diluent, *Chin. J. Chem. Eng.* 28 (2020) 1415–1423.
- [86] D. Kim, H. Vovusha, U. Schwingenschlögl, S.P. Nunes, Polyethersulfone flat sheet and hollow fiber membranes from solutions in ionic liquids, *J. Membr. Sci.* 539 (2017) 161–171.
- [87] N. Ismail, M. Essalhi, M. Rahmati, Z. Cui, M. Khayet, N. Tavajohi, Experimental and theoretical studies on the formation of pure β -phase polymorphs during fabrication of polyvinylidene fluoride membranes by cyclic carbonate solvents, *Green Chem.* 23 (2021) 2130–2147.
- [88] H. Iesavand, M. Rahmati, D. Afzali, S. Modiri, Investigation on adsorption and release of mercaptopurine anticancer drug from modified polylactic acid as polymer carrier by molecular dynamic simulation, *Mater. Sci. Eng. C* 105 (2019) 110010.
- [89] M. Rahmati, M. Jangali, Molecular dynamics simulation of proton conductivity enhancement in polymer membranes by Y-doped BaCeO₃ nanoparticles, *Comput. Mater. Sci.* 169 (2019) 109139.
- [90] N. Ghahramani, M. Rahmati, The effect of the molecular weight and polydispersity index on the thermal conductivity of Polyamide 6: a molecular dynamics study, *Int. J. Heat Mass Tran.* 154 (2020) 119487.
- [91] H. Sun, COMPASS: an ab initio force-field optimized for condensed-phase applications overview with details on alkane and benzene compounds, *J. Phys. Chem. B* 102 (1998) 7338–7364.
- [92] H. Sun, P. Ren, J. Fried, The COMPASS force field: parameterization and validation for phosphazenes, *Comput. Theor. Polym. Sci.* 8 (1998) 229–246.
- [93] M. Khayet, G. Chowdhury, T. Matsuura, Surface modification of polyvinylidene fluoride pervaporation membranes, *AIChE J.* 48 (2002) 2833–2843.
- [94] A. Bottino, G. Capannelli, S. Munari, A. Turturro, Solubility parameters of poly(vinylidene fluoride), *J. Polym. Sci. B Polym. Phys.* 26 (1988) 785–794.
- [95] M.A. Rasool, P.P. Pescarmona, I.F.J. Vankelecom, Applicability of organic carbonates as green solvents for membrane preparation, *ACS Sustain. Chem. Eng.* 7 (2019) 13774–13785.
- [96] D.W. van Krevelen, K. te Nijenhuis, *Properties of Polymers: Their Correlation with Chemical Structure; Their Numerical Estimation and Prediction from Additive Group Contributions*, Elsevier Science, 2009.
- [97] Y. Zhang, X. Wang, Z. Cui, E. Drioli, Z. Wang, S. Zhao, Enhancing wetting resistance of poly(vinylidene fluoride) membranes for vacuum membrane distillation, *Desalination* 415 (2017) 58–66.
- [98] Y. Dai, J. van Spronsen, G.-J. Witkamp, R. Verpoorte, Y.H. Choi, Natural deep eutectic solvents as new potential media for green technology, *Anal. Chim. Acta* 766 (2013) 61–68.
- [99] A.P. Abbott, G. Capper, D.L. Davies, R.K. Rasheed, V. Tambyrajah, Novel solvent properties of choline chloride/urea mixtures, *Chem. Commun.* (2003) 70–71.
- [100] M.K. Hadj-Kali, K.E. Al-khidir, I. Wazeer, L. El-blidi, S. Mulyono, I.M. AlNashef, Application of deep eutectic solvents and their individual constituents as surfactants for enhanced oil recovery, *Colloids Surf. A Physicochem. Eng. Asp.* 487 (2015) 221–231.
- [101] A. Anvari, A. Safekordi, M. Hemmati, F. Rekabdar, M. Tavakolmoghadam, A. Azimi Yancheshme, A. Gheshlaghi, Enhanced separation performance of PVDF/PAN blend membrane based on PVP tuning, *Desalination Water Treat.* 57 (2016) 12090–12098.
- [102] S. Mohsenpour, A. Safekordi, M. Tavakolmoghadam, F. Rekabdar, M. Hemmati, Comparison of the membrane morphology based on the phase diagram using PVP as an organic additive and TiO₂ as an inorganic additive, *Polymer* 97 (2016) 559–568.
- [103] B.J. Cha, J.M. Yang, Effect of high-temperature spinning and PVP additive on the properties of PVDF hollow fiber membranes for microfiltration, *Macromol. Res.* 14 (2006) 596–602.
- [104] Q. Wei, Y. Zhang, Y. Wang, W. Chai, M. Yang, Measurement and modeling of the effect of composition ratios on the properties of poly(vinyl alcohol)/poly(vinyl pyrrolidone) membranes, *Mater. Des.* 103 (2016) 249–258.
- [105] X. Cai, T. Lei, D. Sun, L. Lin, A critical analysis of the α , β and γ phases in poly(vinylidene fluoride) using FTIR, *RSC Adv.* 7 (2017) 15382–15389.
- [106] R. Gregorio Jr., Determination of the α , β , and γ crystalline phases of poly(vinylidene fluoride) films prepared at different conditions, *J. Appl. Polym. Sci.* 100 (2006) 3272–3279.
- [107] J.-J. Qin, F.-S. Wong, Y. Li, Y.-T. Liu, A high flux ultrafiltration membrane spun from PSU/PVP (K90)/DMF/1,2-propanediol, *J. Membr. Sci.* 211 (2003) 139–147.
- [108] H.H. Wang, J.T. Jung, J.F. Kim, S. Kim, E. Drioli, Y.M. Lee, A novel green solvent alternative for polymeric membrane preparation via nonsolvent-induced phase separation (NIPS), *J. Membr. Sci.* 574 (2019) 44–54.
- [109] Z. Wang, H. Yu, J. Xia, F. Zhang, F. Li, Y. Xia, Y. Li, Novel GO-blended PVDF ultrafiltration membranes, *Desalination* 299 (2012) 50–54.
- [110] J. Zhang, Z. Xu, W. Mai, C. Min, B. Zhou, M. Shan, Y. Li, C. Yang, Z. Wang, X. Qian, Improved hydrophilicity, permeability, antifouling and mechanical performance of PVDF composite ultrafiltration membranes tailored by oxidized low-dimensional carbon nanomaterials, *J. Mater. Chem.* 1 (2013) 3101–3111.
- [111] T. Wu, B. Zhou, T. Zhu, J. Shi, Z. Xu, C. Hu, J. Wang, Facile and low-cost approach towards a PVDF ultrafiltration membrane with enhanced hydrophilicity and

- antifouling performance via graphene oxide/water-bath coagulation, *RSC Adv.* 5 (2015) 7880–7889.
- [112] X. Zhao, H. Xuan, A. Qin, D. Liu, C. He, Improved antifouling property of PVDF ultrafiltration membrane with plasma treated PVDF powder, *RSC Adv.* 5 (2015) 64526–64533.
- [113] M. Safarpour, A. Khataee, V. Vatanpour, Preparation of a novel polyvinylidene fluoride (PVDF) ultrafiltration membrane modified with reduced graphene oxide/titanium dioxide (TiO₂) nanocomposite with enhanced hydrophilicity and antifouling properties, *Ind. Eng. Chem. Res.* 53 (2014) 13370–13382.
- [114] F. Liu, M.R.M. Abed, K. Li, Preparation and characterization of poly(vinylidene fluoride) (PVDF) based ultrafiltration membranes using nano γ -Al₂O₃, *J. Membr. Sci.* 366 (2011) 97–103.
- [115] W. Li, X. Sun, C. Wen, H. Lu, Z. Wang, Preparation and characterization of poly(vinylidene fluoride)/TiO₂ hybrid membranes, *Front. Environ. Sci. Eng.* 7 (2013) 492–502.
- [116] K.H. Lasisi, W. Yao, T.F. Ajibade, H. Tian, F. Fang, K. Zhang, Impacts of sulfuric acid on the stability and separation performance of polymeric PVDF-based membranes at mild and high concentrations: an experimental study, *Membranes* 10 (2020) 375.
- [117] Y. Jin, Y. Hua, P. Zhang, Y. Yun, P. Zhang, C. Li, Preparation and characterization of poly(vinylidene fluoride) ultrafiltration membrane with organic and inorganic porogens, *Desalination* 336 (2014) 1–7.
- [118] Z. Zhao, J. Zheng, M. Wang, H. Zhang, C.C. Han, High performance ultrafiltration membrane based on modified chitosan coating and electrospun nanofibrous PVDF scaffolds, *J. Membr. Sci.* 394–395 (2012) 209–217.
- [119] L. Chen, Y. Si, H. Zhu, T. Jiang, Z. Guo, A study on the fabrication of porous PVDF membranes by in-situ elimination and their applications in separating oil/water mixtures and nano-emulsions, *J. Membr. Sci.* 520 (2016) 760–768.
- [120] Y. Zhang, P. Liu, Preparation of porous ZrO₂ solid superacid shell/void/TiO₂ core particles and effect of doping them on PVDF membranes properties, *Chem. Eng. Sci.* 135 (2015) 67–75.
- [121] Q. Li, Q.-y. Bi, H.-H. Lin, L.-X. Bian, X.-L. Wang, A novel ultrafiltration (UF) membrane with controllable selectivity for protein separation, *J. Membr. Sci.* 427 (2013) 155–167.
- [122] C.S. Ong, W.J. Lau, P.S. Goh, B.C. Ng, T. Matsuura, A.F. Ismail, Effect of PVP molecular weights on the properties of PVDF-TiO₂ composite membrane for oily wastewater treatment process, *Separ. Sci. Technol.* 49 (2014) 2303–2314.
- [123] C.S. Ong, W.J. Lau, P.S. Goh, B.C. Ng, A.F. Ismail, Preparation and characterization of PVDF-PVP-TiO₂ composite hollow fiber membranes for oily wastewater treatment using submerged membrane system, *Desalination Water Treat.* 53 (2015) 1213–1223.
- [124] T. Rajasekhar, M. Trinadh, P. Veera Babu, A.V.S. Sainath, A.V.R. Reddy, Oil–water emulsion separation using ultrafiltration membranes based on novel blends of poly(vinylidene fluoride) and amphiphilic tri-block copolymer containing carboxylic acid functional group, *J. Membr. Sci.* 481 (2015) 82–93.
- [125] E. Yuliwati, A.F. Ismail, Effect of additives concentration on the surface properties and performance of PVDF ultrafiltration membranes for refinery produced wastewater treatment, *Desalination* 273 (2011) 226–234.
- [126] L. Yan, S. Hong, M.L. Li, Y.S. Li, Application of the Al₂O₃-PVDF nanocomposite tubular ultrafiltration (UF) membrane for oily wastewater treatment and its antifouling research, *Separ. Purif. Technol.* 66 (2009) 347–352.
- [127] M. Liu, J. Li, Z. Guo, Polyaniline coated membranes for effective separation of oil-in-water emulsions, *J. Colloid Interface Sci.* 467 (2016) 261–270.
- [128] H. Shi, Y. He, Y. Pan, H. Di, G. Zeng, L. Zhang, C. Zhang, A modified mussel-inspired method to fabricate TiO₂ decorated superhydrophilic PVDF membrane for oil/water separation, *J. Membr. Sci.* 506 (2016) 60–70.
- [129] X. Huang, W. Wang, Y. Liu, H. Wang, Z. Zhang, W. Fan, L. Li, Treatment of oily waste water by PVP grafted PVDF ultrafiltration membranes, *Chem. Eng. J.* 273 (2015) 421–429.
- [130] J. Liu, P. Li, L. Chen, Y. Feng, W. He, X. Lv, Modified superhydrophilic and underwater superoleophobic PVDF membrane with ultralow oil-adhesion for highly efficient oil/water emulsion separation, *Mater. Lett.* 185 (2016) 169–172.
- [131] F.O. Agyemang, F. Li, F.W.Y. Momade, H. Kim, Effect of poly(ethylene oxide) and water on electrospun poly(vinylidene fluoride) nanofibers with enhanced mechanical properties as pre-filter for oil-in-water filtration, *Mater. Chem. Phys.* 182 (2016) 208–218.
- [132] M.A. Masuelli, Ultrafiltration of oil/water emulsions using PVDF/PC blend membranes, *Desalination Water Treat.* 53 (2015) 569–578.
- [133] L.Y. Susan, S. Ismail, B.S. Ooi, H. Mustapa, Surface morphology of pvdf membrane and its fouling phenomenon by crude oil emulsion, *J. Water Proc. Eng.* 15 (2017) 55–61.
- [134] Regulation (EC) No 1272/2008 of the European Parliament and of the Council of 16 December 2008, in: *Official Journal of the European Union*, 2008. <https://eur-lex.europa.eu/legal-content/EN/TXT/PDF/?uri=CELEX:32008R1272&from=BG>.
- [135] P. Yadav, N. Ismail, M. Essalhi, M. Tysklind, D. Athanassiadis, N. Tavajohi, Assessment of the environmental impact of polymeric membrane production, *J. Membr. Sci.* 622 (2021) 118987.
- [136] MSDS Europe, 2015. <https://www.msds-europe.com/r-phrases-s-phrases/>.
- [137] Globally Harmonized System of Classification and Labelling of Chemicals (GHS), Fifth revised edition, 2013. <https://unece.org/ghs-rev5-2013>.